Inhaled Nitric Oxide: An Experimental Analysis of Continuous Flow Noninvasive Delivery via Nasal Cannula

By

Kineshta Pillay

A thesis submitted in partial fulfillment of the requirements for the degree of

Master of Science

Department of Mechanical Engineering

University of Alberta

©Kineshta Pillay, 2020

Abstract

Inhaled nitric oxide (iNO) is used to treat pulmonary hypertension and improve oxygenation in critically ill patients. It is primarily delivered via mechanical ventilation to patients in the critical care setting; however, there are several drawbacks to this invasive form of delivery. As a result, there has been increased administration of noninvasive delivery in the critical care setting, as well as investigation into long-term noninvasive administration of iNO to treat pulmonary hypertension associated with chronic lung diseases. Dose delivery of iNO is currently defined in terms of the constant concentration that is maintained in the inspired gas although applying this metric for delivery modes other than ventilation is challenging. Dose delivery for iNO supplied at a constant flow rate through a nasal cannula has not yet been established. This thesis aims to determine the influence of nasal cannula type, supply flow rates, and the patient's breathing pattern on delivered iNO through a nasal cannula. Additionally, a basis for dosage estimation through this delivery mode is provided. This assessment was conducted *in vitro* using a realistic adult airway replica and lung simulator.

The first chapter of this thesis examines and reviews the literature around the applications of iNO and its delivery methods. Chapter 2 examines the theoretical basis for this experimental study of iNO, while the study design and results of experiments are provided in Chapter 3. Chapter 4 summarizes the thesis and provides perspectives for future work.

In the experiments conducted, carbon dioxide (CO_2) was used as a tracer gas to mimic the delivery of nitric oxide at a continuous flow rate. It was supplied through a nasal cannula to a realistic adult nose-throat airway replica. This replica was connected to a lung simulator that imposed breathing patterns representative of patients during rest, sleep and light exercise. A canister of soda lime was used in the system to mimic NO absorption in the lung. CO_2 flows were selected to provide targeted tracheal concentrations at rest of 5 or 20 parts per million (ppm) NO and were initially supplied with 2 L/min of supplemental oxygen (O_2). Three different cannulas were tested, followed by additional tests with 6 L/min oxygen supply at both CO_2 flows. Breathing patterns were later varied to investigate tidal volume and breathing frequency influences independently. Dosage delivery was presented in the form of tracheal NO concentrations, along with NO mass flow rate past the trachea. Delivery efficiency was assessed for each condition and presented an estimate of the NO that was delivered to the trachea in relation to the NO supplied. Delivery results, tracheal NO concentrations and mass flow rates, were compared to predictive equations to determine whether dosage delivery could be reasonably quantified for future applications.

Tracheal NO concentrations differed significantly based on breathing pattern and supply flow rates. However, for the same test conditions, mass flow rate of NO past the trachea was notably less sensitive to breathing pattern. Provided breathing parameters were known, inhaled tracheal NO concentrations were reasonably predicted using a simple assumption of complete mixing of the NO flow within the inspired breath. Cannula type had a minimal effect on inhaled NO concentrations and mass flow rate. Mass flow rate and delivery efficiency increased when overall minute volume increased. Due to the low variation in delivery across breathing pattern, mass flow rate could provide a stable option

as a delivery metric for iNO. The presented information describing inhaled NO concentration, mass flow and delivery efficiency will help in establishing NO dosing for noninvasive continuous flow delivery.

Preface

This thesis contains some work that has been co-authored and will be submitted for publication. Chapter 3 was a co-authored manuscript for which I was the primary author and will be submitted for publication in a scientific journal. The co-authors who will be included on the manuscript are John Z. Chen, Dr. Warren H. Finlay and Dr. Andrew Martin. The LabVIEW code used for recording experimental data and the Excel spreadsheet used to extract information from the raw data were adapted from those provided by John Z. Chen who established them for work on continuous oxygen delivery. I was responsible for building the experimental set-up used in Chapter 3, as well as data collection and analysis. The drafting of this manuscript was my responsibility with significant editorial support, direction and contributions from Dr. Martin, especially for Chapter 3.

To my parents,

Ananthan and Mayesveri Gopal Pillay,

whose sacrifices, love, and strength have shaped me into the person I am today.

Acknowledgements

I'd first like to thank my supervisor Dr. Andrew Martin, who changed my life by offering me an opportunity to pursue graduate studies in this field. Your guidance, patience and support have been invaluable and I am eternally grateful for having had a supervisor who I so enjoy working with, and who has his students' best interests at heart. This period in my life has been the most rewarding, and no small part of it has been as a result of your dependability and help navigating the difficulties of grad school, careers and studies. Thank you for guiding me, both as a young researcher and graduate student. Your insight and mentorship have made all the difference and I can think of no better role model in this time than you.

I would also like to express my gratitude to Dr Warren Finlay and Dr Alexandra Komrakova, both for your contributions as part of my examination committee and during my studies. Your feedback and time are greatly appreciated.

I would like to thank all the members of the aerosol research lab and respiratory mechanics lab for their support during my time here. John Chen, I am so grateful for your guidance with setting up my experiments and explaining the data processing procedure to me. Your help and patience, even helping me troubleshoot when I had difficulties with the equipment, is greatly appreciated. Tyler Paxman and Kelvin Duong, thank you for your support and advice, both with coursework and just as friends. To Scott Tavernini and Conor Ruzycki, thank you for your help navigating the labs and for your readiness to help me figure out what I needed when setting up apparatuses. Finally, I would like to thank Paul Moore. I have been so fortunate to have had your support first as a colleague, then as a friend and finally as a partner. You have made a world of difference to my

development in this time, both as a researcher and as a person. I am so grateful to have had you at my side.

I would not be who (or where) I am today without my incredible family and friends. Thank you to my wonderful siblings Yashodani and Sobhithan Pillay for being not just family, but friends too, and for help with everything from teaching me about mechanistic responses to taking care of me when I was stressed. Thank you to Shamla Govender and Nugalen Pillay for all the support and being like second parents to me. Thank you to my grandmothers, Lillavathi and Velliamma Pillay, for the love and support from halfway across the world, and for being such strong women who've always encouraged my education and independence. I'm grateful for my cousins Neryvia, Vedarsharn, Sarteyan, Prineesa, Marica, Yaazhin and Kumaresan and all the support from afar that you've given me. A day doesn't go by when I don't miss you all. I'm also incredibly lucky to have friends who are so patient and compassionate, who readily reach out to support me at the drop of a hat, even though I'm so far away. Thank you for all the love Kelby, Killiann, Kaveer, Shenelle and Darren. You have made the hard times so much more bearable.

Finally, I would like to acknowledge the financial support from the Natural Sciences and Engineering Research Council of Canada (NSERC). Their generous financial support made the work in this thesis possible.

Kineshta Pillay

November 29th, 2019

Edmonton, AB, Canada

Table of Contents

List of Tables

List of Figures

Chapter 1 Introduction

1.1 Overview

Inhaled nitric oxide therapy, often referred to as iNO, is used as a selective pulmonary vasodilator. It is used as treatment for a range of respiratory issues, from alleviating pulmonary hypertension in newborns, to improving oxygenation in adults (DiBlasi, Myers, & Hess, 2010, Griffiths and Evans, 2005). Inhaled NO is conventionally delivered through mechanical ventilation in the critical care setting, but long-term ambulatory applications are also being investigated. The NO gas is typically delivered simultaneously with oxygen, injected as a constant concentration into a flow that adapts to the patient's breathing pattern. In addition, there have been some studies showing that a high concentration bolus of iNO delivered early in the patient's breath can have comparably positive results (Ivy *et al*., 2003, Robyn J. Barst *et al*., 2012).

Mechanical ventilation (an invasive system) as the primary means of delivery limits the use of iNO therapy outside of the critical care setting. As such, there has been exploration into the use of noninvasive delivery methods for iNO therapy. Currently, the least invasive form of medical gas delivery is through a nasal cannula; however, the open interface makes controlling delivery challenging. Delivery of iNO through a nasal cannula has produced positive haemodynamic results such as reduced pulmonary vascular resistance and increased cardiac output (Tremblay *et al*., 2019). However, in order to provide accurate and safe dosing for noninvasive iNO treatment, further investigation into delivery of therapy through a nasal cannula is required.

1.2 Purpose of Research

It is the objective of this thesis to investigate how iNO delivery at a constant flow rate through a nasal cannula is influenced by a variation in delivery parameters. Despite the simplicity of this delivery method, there has been little investigation into it. In order to remedy this, this thesis seeks to provide a basis for dosage estimates as well as an assessment of the feasibility of this delivery method. This was achieved *in vitro* by evaluating continuous flow iNO delivery to a realistic adult airway replica. The influence of cannula design, supply flow rates of both iNO and supplementary oxygen, and the patient's respiratory pattern are all explored.

The current dose metric for iNO therapy describes the delivered dose in terms of concentration of NO in the inspired gas; however, doses delivered across open interfaces change as a result of simultaneous air entrainment from the surroundings. The research in this thesis is presented across multiple dose metrics and provides iNO dosage delivery estimates for inhaled gas arriving at the trachea. In addition, the efficiency of the delivery mechanism is assessed along with a set of predictive comparisons for delivery. These results could help to facilitate noninvasive iNO treatment and provide a basis for further investigation into use of iNO outside of the intensive care environment.

1.3 Thesis Structure

This thesis is presented over four chapters. The present (first) chapter presents an overview of existing literature and research in this field. This ranges from the clinical applications of inhaled nitric oxide to the various delivery mechanisms through which treatment is provided. The second chapter provides an overview of the literature that informed the experimental design. This overview is then translated into the specific

equations and methodology implemented during the investigative portion of the work. The third chapter is presented in the format in which it will be submitted for publication. In the study outlined in this chapter a realistic airway model was connected to a mechanical lung simulator to simulate the breathing of an adult human. Varying flow rates of nitric oxide and supplemental oxygen were supplied through different types of nasal cannulas to the airway replica. Tracheal dose delivery and efficiency of delivery through the cannulas is presented. The fourth and final chapter summarizes the research findings and discusses potential avenues for further investigation into iNO delivery.

1.4 Literature Review

1.4.1 Clinical Application of Inhaled Nitric Oxide

Physiological mechanism of iNO

Inhaled nitric oxide (iNO) is an endothelium-derived relaxing factor that is used in a variety of clinical settings as a selective pulmonary vasodilator (C. Frostell *et al*., 1991). The role of endogenous NO as a signalling molecule in the cardiovascular system was discovered in the 1980s and its pioneers were awarded the Nobel Prize in Medicine in 1998. Inhaled nitric oxide regulates vascular muscle tone and increases blood flow to areas of the lungs with normal ventilation/perfusion ratios by dilating pulmonary vessels in better-ventilated regions (C. G. Frostell *et al*., 1993, Luscher, T. F. and Vanhoutte, P. M., 1988, Robyn J. Barst *et al*., 2012). When delivered via inhalation, nitric oxide that reaches the lung is rapidly absorbed. It diffuses across the alveolar-capillary membrane and binds to haemoglobin. As such, it's results are localized to the respiratory system and have little effect on systemic circulation (DiBlasi *et al*., 2010, S. Lundin and Stevqvist, 1997, Robyn J. Barst *et al.*, 2012).

Respiratory conditions treated by iNO therapy

Inhaled nitric oxide is currently indicated to treat term/near-term neonates with hypoxic respiratory failure linked to pulmonary hypertension and is used primarily to treat persistent pulmonary hypertension of the newborn (PPHN) (Kumar, 2014). PPHN is associated with increased pulmonary vascular resistance (PVR), mismatched ventilation-perfusion and right-to-left cardiac shunting resulting in system hypoxia (Bin-Nun and Schreiber, 2008, Kanmaz *et al*., 2017). Inhaled NO has been proven to alleviate the symptoms of PPHN, leading to improved arterial oxygenation and hemodynamic stability (DiBlasi *et al*., 2010). In addition, it is used to improve PVR in adults with complications associated with pulmonary hypertension, such as chronic obstructive pulmonary disease (COPD) (Ashutosh *et al*., 2000), as well as to improve oxygenation in patients with acute respiratory distress syndrome (ARDS) or acute lung injury (Creagh-Brown, Griffiths, & Evans, 2009, Griffiths and Evans, 2005). The use of iNO for patients with acute lung injury (characterized by mild pulmonary hypertension) has been linked with a small decrease in pulmonary arterial pressure (PAP). The decrease in PAP as a result of iNO therapy has supported its use as part of perioperative treatment for acute right ventricular dysfunction associated with cardiac surgery both in adults and children (Auler Júnior *et al*., 1996, Checchia, Bronicki, & Goldstein, 2012, Oz and Ardehali, 2004, Tremblay *et al*., 2019).

Exploratory applications of iNO

Due the benefits of iNO therapy on the pulmonary vascular system, there has been further exploratory investigation into treatments for other associated conditions. One of these conditions is pulmonary arterial hypertension (PAH), a chronic progressive disease of the pulmonary vascular system causing right ventricular failure and, if left untreated, death

(Robyn J. Barst *et al.*, 2012). Since PAH is a chronic condition, there has been investigation into treatment that can improve the quality of life of those diagnosed while minimizing potential side effects. Inhaled nitric oxide, often combined with oxygen therapy, has been explored as a solution and is also used as a diagnostic tool in the evaluation of PAH patients (Barst *et al*., 2010, McLaughlin *et al*., 2009). As such, there has been research into improving iNO delivery mechanisms for long-term ambulatory applications (Abman, 2013, Kinsella *et al*., 2003, Robyn J. Barst *et al*., 2012). Other exploratory investigations of iNO include it's use as an anti-microbial agent (Schairer *et al*., 2012), particularly for the treatment of Mycobacterium infections in cystic fibrosis patients (Yaacoby-Bianu *et al*., 2018).

Other pulmonary vasodilators

Nitric oxide is not the only pulmonary vasodilator used for treatment of these respiratory conditions. Several drugs such as epoprostenol, iloprost and prostaglandin are used to treat pulmonary hypertension (Griffiths and Evans, 2005). In addition, there are medications that are used in conjunction with iNO to get specific outcomes. Orally administered sildenafil, for example, has been combined with iNO therapy to provide synergistic pulmonary vasodilation and there has been investigation into further treatment for PPHN (Kanmaz *et al*., 2017). A significant benefit of iNO over other administered drugs is that treatment is selective to the respiratory system and there are no reported side effects outside of it. While studies have shown several benefits of iNO treatment both in acute applications in an intensive care setting and during long term therapy, it should be noted that there have been concerns about rebound phenomena when iNO treatment is discontinued, and no consistent improvements in mortality rates have been demonstrated (DiBlasi *et al*., 2010, Griffiths and Evans, 2005, Westphal, K. *et al*., 1998).

1.4.2 Inhaled Nitric Oxide Delivery

Inhaled NO therapy is provided to patients primarily in the intensive care setting where it is delivered through mechanical ventilation. These patients, supported by positive pressure ventilation (either invasive or noninvasive), receive 1 - 80 parts per million (ppm) of iNO, depending on the clinical end point being targeted (Bhatraju *et al*., 2015). There are several advantages to this delivery method; however, patient discomfort from mechanical ventilation, whether delivered through an endotracheal tube or a tight-fitting facemask, is a strong motivation to explore noninvasive forms of delivery.

Mechanical Ventilation

Prior to the late 1990s iNO was supplied through ventilatory systems that provided a constant concentration through a time-cycled continuous flow mechanism (DiBlasi *et al*., 2010). Imanaka *et al*. outlined several drawbacks of these ventilators, including difficulties with constant concentrations of NO in continuous flow. Providing an inspired iNO concentration that was both accurate and safe was challenging, and this delivery sometimes resulted in tracheal iNO concentrations an order of magnitude greater than the target concentration of the supplied gas (Imanaka *et al*., 1997). Other problems included ventilator failure, ventilator trigger issues and tidal volume augmentation (DiBlasi *et al.*, 2010, Hess, Ritz, & Branson, 1997, Imanaka *et al*., 1997). Since then NO delivery devices for ventilators have adapted. Current devices proportionally adjust the rate that source NO-containing gas is injected into the ventilator breathing circuit. These adjustments are determined by changes in the patient's respiratory pattern to ensure that a constant NO concentration in the inhaled gas mixture is maintained (Imanaka *et al.*, 1997, S. Lundin and Stevqvist, 1997, Young, Roberts, & Gale, 1997).

The source NO-containing gas in the ventilator circuit is typically supplied from a gas cylinder containing 800 ppm NO, in nitrogen (N_2) in North America, or 225-1000 ppm NO/N_2 in Europe (Martin *et al*., 2016). It is supplied to one of the devices that are currently commercially available to administer iNO through delivery and control of flow through the ventilator. These devices inject NO into the inspiratory limb of the ventilator, as shown in Figure 1-1, while regulating the flow according to changes in the ventilator waveforms to provide a constant inspired concentration of NO to the patient intake (Young *et al*., 1997). In addition, they continuously monitor the inspired concentrations of NO, O_2 and nitrogen dioxide.

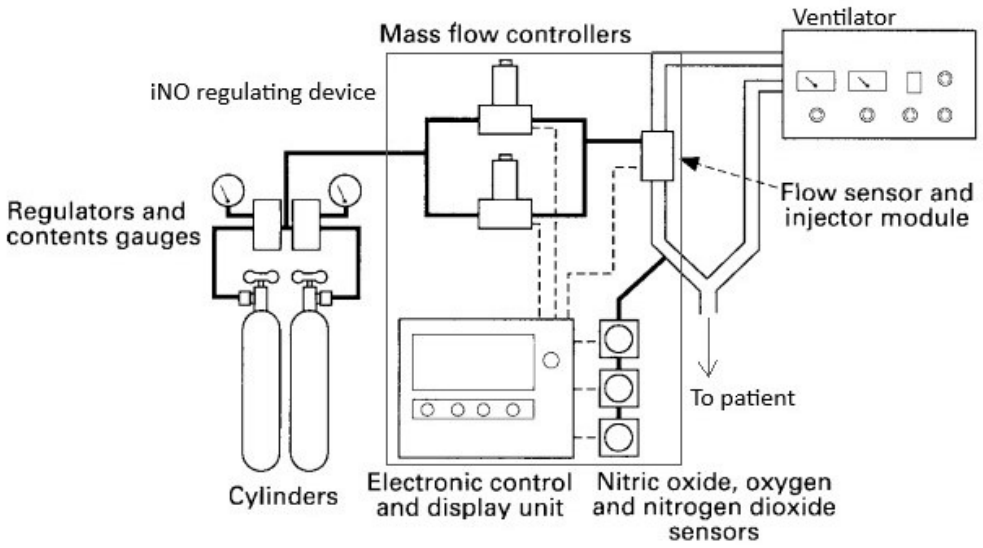

Figure 1-1 Adapted from Young et al. this schematic shows the set up for a ventilator system using a proportional flow iNO injection device. The large box indicates the components that make up the device that is used to regulate iNO in the ventilation system connected to the patient.

Nitrogen dioxide (NO_2) is a toxic by-product that forms when NO and O_2 interact. This reaction can occur during the gas delivery, in the ventilator, the airway interface or the lungs (DiBlasi *et al*., 2015). Although the Occupational Safety and Health Administration

limits human peak exposure to 5 ppm (Centers for Disease Control, 1988), studies have shown adverse effects from inhalation of NO_2 concentrations as low as 2 ppm, including decreased alveolar permeability (Rasmussen *et al*., 1992) and varying airway responsiveness (Bylin *et al*., 1987). NO_2 generation is influenced by several factors including the fraction of inspired oxygen in the inhaled gas, dose of iNO, and residence time in the system for iNO and oxygen (Lindberg and Rydgren, 1999).

Since the concentrations of NO, O_2 and NO_2 could all have adverse effects at the wrong magnitude, monitoring them during NO delivery is vital. Mechanical ventilator systems that monitor gas mixing have fewer drawbacks than older continuous flow ventilatory systems. Inhaled nitric oxide is also delivered through ventilatory systems such as manual ventilation when mechanical ventilation has failed, or in conjunction with inhaled anaesthetic gases using an anaesthetic ventilator. Anaesthetic ventilation supplemented with iNO is sometimes applied during or after cardiac surgery in infants with pulmonary hypertension. A circle or partial rebreathing system is used to allow patients to breathe a combination of fresh and exhaled gas (DiBlasi *et al*., 2010). In order to preserve the aggregate anaesthetic carbon dioxide (CO_2) in the exhaled gas is eliminated from the breathing circuit through an absorption agent such as soda lime before circling back to the patient's intake.

Noninvasive delivery

Although mechanical ventilation has proven an effective means of delivering iNO to patients who are critically ill, there has been a shift towards investigation into noninvasive delivery. One of the concerns about invasive ventilation is the incidence of volutrauma

(distortion of the alveoli) and potential increase of the body's inflammatory cascade (Smith and Perez, 2016), a systemic inflammatory response. Noninvasive delivery can alleviate these concerns, in addition to improving patient comfort and facilitating ambulatory long-term treatment. While there has been significant research conducted into delivery optimization for the invasive delivery applications of iNO, noninvasive delivery is still under investigation. Noninvasive delivery often poses the challenge of delivering safe and effective doses of iNO to patients without the control that delivery through invasive ventilation can provide. Open interfaces, such as a nasal cannula, make control and prediction of delivery particularly difficult, as the amount of room air inhaled together with delivered gases will vary as the patient breathes.

There are several options for noninvasive delivery interfaces of iNO including simple facemasks, nasal cannulas (both high and low flow) and noninvasive ventilatory devices (NIV). Figure 1-2 shows the different level of control and comfort in relation to the invasiveness, or lack thereof, of the aforementioned devices. NIV is an interface that falls somewhere between invasive ventilation and simpler open interfaces; however, as it requires a ventilation system to function and incorporates a tight-fitting facemask, it is not applicable for long-term treatment. As with invasive ventilation, noninvasive delivery has different applications depending on the type of the clinical application as well as individual patient needs. Multiple studies have shown positive hemodynamic effects of noninvasive interfaces, including for treatment of PAH, ARDS, PPHN and PH secondary to COPD (Abman, 2013, DiBlasi *et al*., 2015, Ivy *et al*., 1998, Ivy *et al*., 2003, Kinsella *et al*., 2003, Smith and Perez, 2016, Tremblay *et al*., 2019). The use of noninvasive delivery mechanisms for iNO treatment has increased over the years while conventional mechanical ventilation has decreased (Vendettuoli *et al*., 2014). As a result of further

investigation into noninvasive delivery, there has been exploration into control and improvement of dose delivery.

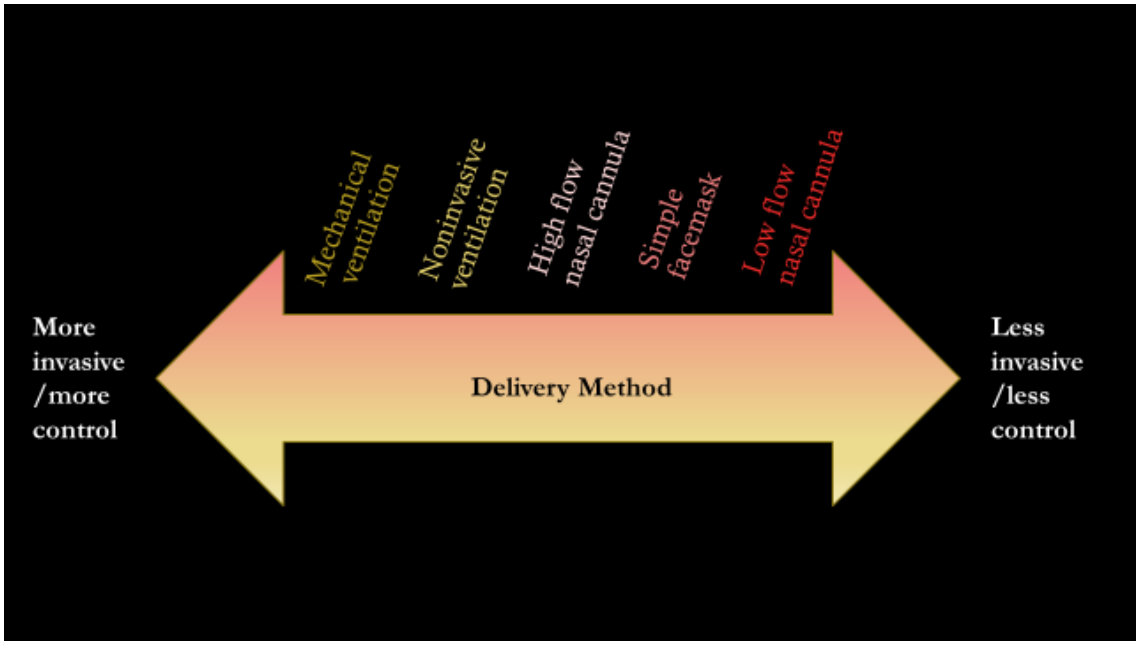

Figure 1-2 Delivery interfaces ranging from most to least invasive are displayed. While more invasive mechanisms tend to provide more controlled delivery of iNO, less invasive devices tend to provide more comfort and mobility to patients.

Control of iNO delivery

The current standard approach for delivery of iNO is through a constant inspired concentration. For delivery through the proportional flow systems used for mechanical ventilation this delivery method is effective. However, there are several complications when using this delivery method for noninvasive systems, particularly when the delivery interface is an open one. In order to maintain a constant iNO concentration in the inhaled gas, very high flow rates in excess of patient inspiratory flow rates would need to be administered. However, this approach is inefficient and has the potential of contaminating the room air with NO and NO_2, thereby producing an unsafe environment for others in the shared space. An alternative would be to inject the iNO into the delivery apparatus in proportion to the patient inspiratory flow rate. This would be challenging as it is difficult

to anticipate the patient's spontaneous breathing timeously to adequately adjust injection concentrations into a system like a nasal cannula. A study conducted by DiBlasi *et al.* found that for a constant iNO concentration supply, delivery across an open interface was poorly predicted (DiBlasi *et al*., 2015). As such, constant concentration delivery would be unsuitable for noninvasive iNO administration through an open interface.

Pulsed flow delivery

Noninvasive delivery using a pulsed flow is an alternative approach that is under investigation. Pulsed flow refers to a delivery method where a pulse or bolus of iNO-containing gas is delivered such that it arrives during the early portion of inhalation. Pulsed delivery has been explored as an option for long-term ambulatory iNO administration (Robyn J. Barst *et al*., 2012), and clinical investigation is ongoing (Quinn, D on behalf of Bellerophon Therapeutics, 2019). By supplying iNO in conjunction with oxygen during the early portion of the breath, delivery of iNO to lung regions that fill relatively quickly during inspiration could be improved thereby potentially improving ventilation perfusion matching (Griffiths and Evans, 2005). Ivy *et al.* reported that short-term low flow nasal pulsed delivery was as effective as mask delivery in lowering PVR and PAP in eight children with PAH (Ivy *et al.*, 1998) and other studies reported favourable results in children and young adults with PAH (Channick, R.N. *et al*., 1996, Ivy *et al*., 2003). It would appear that the feasibility of long-term iNO therapy through pulsed flow is dependent on the following factors (Hajian *et al*., 2016, Ivy *et al.*, 1998, Robyn J. Barst *et al*., 2012):

- Maintaining the appropriate iNO concentration in delivery

- Resulting improvement of hemodynamic derangements by nasal cannula at low flow rates
- Effective delivery of NO through nasal interfaces with minimum release of gas into the surrounding environment
- Minimizing replacement of NO sources

There are currently no devices commercially available that deliver pulsed iNO therapy. While there have been some reported advantages to this delivery method, there are several complications that have made ambulatory treatment devices difficult to develop. The leading advantage of pulsed flow is that iNO is not delivered during exhalation. This decreases the potential danger associated with contaminating room air with NO and NO_2, along with decreasing the frequency of cylinder source replacements as the NO is conserved. While this is more efficient than other delivery options, devices would require advanced technology. In order to deliver iNO in the correct portion of breath, devices must monitor patient breathing – a task made more difficult by the open interface of the nasal cannula. Portable oxygen concentrators and oxygen conserving devices, the comparable oxygen delivery devices intended for long-term oxygen administration, use a pressure trigger to sense the start of patient inspiration for pulsed flow. However, despite decades of pulsed oxygen therapy there have been challenges around reliable triggering, particularly during sleep when inhalation flow rates are low (Chen *et al*., 2017). In addition, companies developing these devices are required to include a statement in accompanying device instructions to inform customers that some respiratory efforts of the patient might not trigger delivery (International Organization for Standardization, 2014). Although these devices have backup delivery settings to ensure administration continues when triggering fails, dosing efficiency in this mode is poor and

irregular. Similarly, pulsed iNO delivery devices developed for ambulatory treatment have these hurdles to overcome and as such, will not be suitable for all patients requiring long-term treatment.

Constant flow delivery

Unlike pulsed flow delivery, constant flow delivery is an inherently simple technique. Continuous or constant flow describes delivery wherein the flow rate of iNO supplied to the patient is constant over time. Source iNO-containing gas is supplied with supplemental oxygen via a nasal cannula at a fixed flow rate and mixes with entrained room air as it travels through the upper airway. As mentioned previously, the open interface of the nasal cannula poses the challenge of unknown dilution of effects from the room air. While this challenge should be alleviated during high flow nasal cannula therapy where supply flow rates exceed the patient inspiratory flow rate, studies have not confirmed this (DiBlasi *et al.*, 2015). In addition, during high flow therapy the majority of iNO supplied during exhalation will be lost to the surrounding environment along with the surplus of the supply during inhalation. This could possibly pose a risk in poorly ventilated spaces and the cylinder source from which the iNO is supplied would require regular replacement. However, low continuous flow rates pose minimal risk of room contamination and have the benefits of patient comfort and ease of delivery.

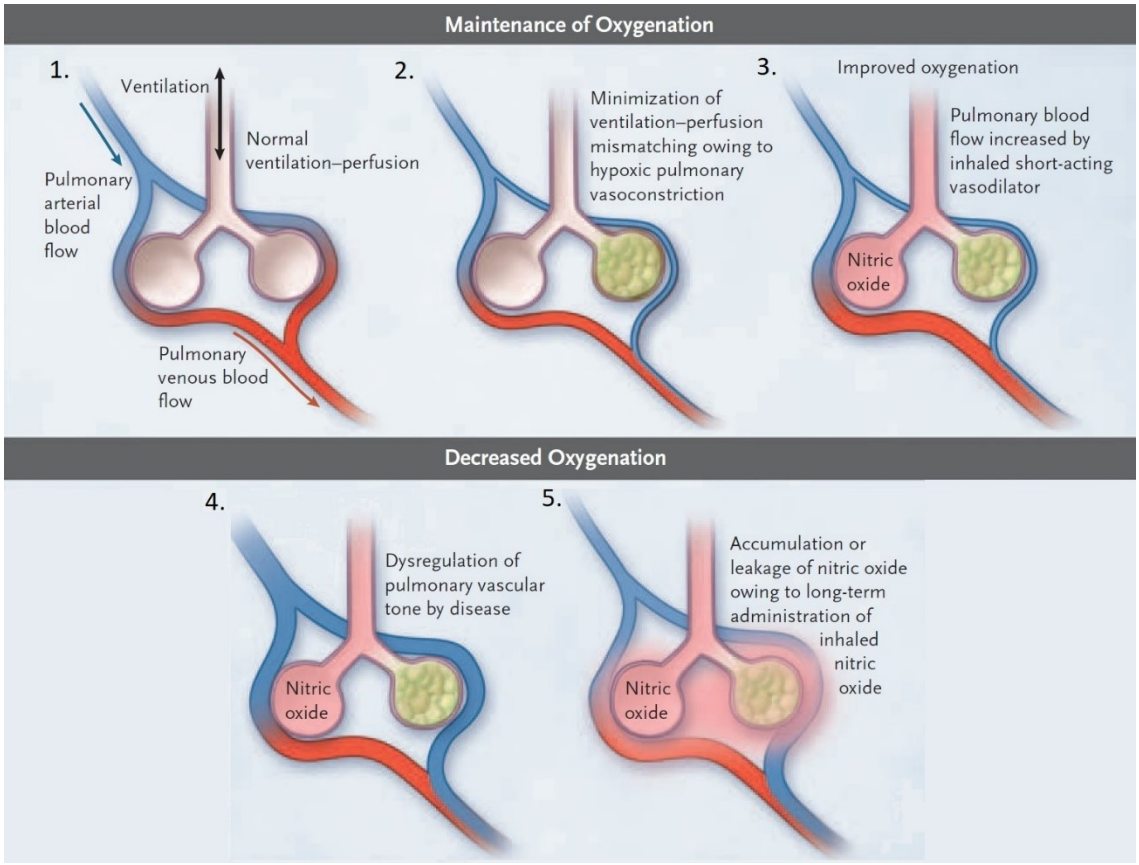

Figure 1-3 Adapted from Griffiths et al., frames 1 - 3 show how ventilation-perfusion in the lungs works ordinarily and how oxygenation is improved by iNO during mismatching (Griffiths and Evans, 2005). However in cases of vasoconstriction in the lungs of people who have experienced some form of lung injury, long-term iNO delivery may cause decreased oxygenation as shown in in frames 4 - 5.

A possible drawback regarding continuous flow relates to ventilation-perfusion mismatching in the lungs being adversely affected by exposure to iNO over a long period of time (Barbera and Roca, 1996, Griffiths and Evans, 2005, Robyn J. Barst *et al.*, 2012). This could potentially reduce overall oxygenation in patients with lung injuries as demonstrated in Figure 1-3. However, the study that found this was delivering high concentrations of iNO to the lungs, and consecutive studies have since found conflicting results (Germann *et al*., 1998, Lundin, S. *et al*., 1999) suggesting that this particular phenomenon may be a concern only under particular circumstances ie. high concentration flows over long periods, to patients with lung damage.

Due to the simple nature of continuous flow delivery, as well as the relative dearth of information linking continuous flow delivery settings (e.g. flow rates) to inhaled doses of NO, further investigation into noninvasive continuous flow delivery is warranted.

1.4.3 Dosing Metrics for Inhaled Nitric Oxide

Dosage is an important consideration in the administration of iNO therapy. Doses that are too large can be harmful to the patient. Conversely, underdosing can be ineffective and possibly result in dangerous rebound effects if succeeding delivery at higher doses. As delivery techniques have evolved, dosing strategies have come under investigation in order to ensure safe and effective NO quantities are administered. Below, dosing is discussed in the context of the three current approaches to dose delivery: constant inspired concentration, pulsed flow delivery, and constant flow delivery.

Constant Concentration Dosing

As previously mentioned, iNO is delivered primarily through ventilation in the critical care environment. It is standard practice in medical gas delivery to report the dose of the gas as inspired concentration (Imanaka *et al*., 1997). Due to advances in the technology, the phrase "constant inspired concentration" in iNO delivery has progressed from implying a fixed concentration delivered continuously regardless of patient breathing patterns, to a constant concentration delivered to the patient by adapting to their breathing. Similar to selection of iNO delivery devices and interfaces, the dose of iNO administered to the patient is dependent on the condition being treated and the patient's needs.

Inspired concentrations of iNO administered for clinical applications typically range from 1 – 80 ppm. These inhaled concentrations are varied based on the condition being treated since haemodynamic results for iNO administration are considered to be dose dependent. For example, while concentrations as low as 2 ppm have been proven to attenuate clinical deterioration in infants (Cornfield *et al*., 1999), it is contested as to whether or not initial treatment using doses this small would preclude a significant improvement in oxygenation when dosage is increased (Cornfield *et al*., 1999, Finer *et al*., 2001). For the treatment of term and near-term infants with hypoxic respiratory failure, a starting dose of 20 ppm iNO is suggested (Barrington *et al*., 2017) while iNO concentrations between 5 and 20 ppm administered to neonates have been shown to improve oxygenation and decrease the necessity for extracorporeal membrane oxygenation (ECMO) therapy in patients with PPHN stemming from a diverse range of conditions (Abman, 2013, Clark *et al.*, 2000, Davidson *et al*., 1998, No Authors, 1997, Roberts *et al*., 1997). Studies in adults and children showed that iNO concentrations of 20 - 40 ppm decreased PAP in cases of cardiac complications complicated by perioperative PAH (Fullerton and McIntyre, 1996). Overall, higher doses of iNO (20 – 80 ppm) are associated with progressive pulmonary vasodilation, while lower doses of iNO (1 - 10 ppm) tend to produce better improvements in oxygenation (Abman, 2013, Fullerton and McIntyre, 1996).

An important factor in dose delivery of inhaled nitric oxide is safety. Inspired concentrations of greater than 80 ppm NO increase the likelihood of adverse effects on the patient through the formation of methaemoglobin (Davidson *et al*., 1998). Methaemoglobin reduces systemic O_2 delivery by interrupting the haemoglobin molecule's capacity to bind with O_2. According to general clinical guidelines, it is

suggested that iNO administration be discontinued if the methaemoglobin level in the patient rises above 5% (DiBlasi *et al*., 2010). Another important consideration linked to safety in long-term iNO dose delivery is the occurrence of rebound hypoxemia and pulmonary hypertension when iNO is discontinued. To prevent this from occurring, patients receiving iNO in the acute setting may be weaned by gradually decreasing the iNO dose to 1 ppm before withdrawal (Abman, 2013, Davidson *et al*., 1999) or through the introduction of a second drug treatment like sildenafil or prostacyclin (Ivy *et al*., 1998, Vonbank *et al*., 2003). Much like the rest of dose administration, treatment for rebound PH should factor in patient characteristics, treatment familiarity, availability, contraindications, supplemental vasodilators and optimal ventilation strategies (Raja, S. G. and Augoustides, J. G., 2004, Robyn J. Barst *et al*., 2012). For accurate and safe delivery, a rapid response analyzer is recommended during administration using this dosing metric to ensure iNO concentrations in the patient do not exceed safety limits (Imanaka *et al*., 1997), although this is not the current practice. While constant concentration in ventilatory systems provides an adequate method of dose delivery for acute clinical treatment and ensures that the iNO concentrations that reach the airways are safe, this is a closed system - unlike those being investigated for noninvasive applications, including long-term ambulatory applications.

Pulsed Flow Dosing

Constant inspired concentration translates poorly into dose delivery for pulsed and intermittent flow devices. For example, a bolus of iNO of a concentration as high as 1000 ppm delivered during the early portion of inspiration might result in similar pulmonary vasodilation as a 5 ppm dose supplied continuously (Heinonen, Hogman, & Merilainen, 2000). This seems non-intuitive and makes prediction for this dose metric challenging;

due to the inherently different dosing strategy, it would be more appropriate to use a different dose metric to describe the iNO that is delivered to the patient. When comparing intermittent flow ventilation systems to continuous ones, Imanaka *et al.* suggested that NO dosage instead be measured in volume of administered iNO since iNO delivery to the lungs may be affected by tidal volume and inspiratory time (Imanaka *et al*., 1997) and NO uptake from the lungs is limited by diffusion (Meyer and Piiper, 1989). Several studies investigating both long-term outpatient administration and short-term inpatient treatment using pulsed nasal delivery, measured iNO dosage in terms of flow rate ie. mL/breath or L/min (Channick, R.N. *et al.*, 1996, Ivy *et al.*, 2003, Kitamukai *et al.*, 2002).

NO uptake in the lung and the NO diffusion constant rely on the surface area and thickness of the diffusive barrier, which in turn depend on patient size (Heinonen *et al*., 2000) so it is reasonable to expect patient size to have an impact on dosage. In a study comparing a simplistic pulsed flow delivery system and mechanical ventilation with a constant inspired concentration of 5 ppm iNO, Heinonen *et al.* found that there was poor correlation between the delivery parameters and NO uptake in the lung, and suggested that NO delivery descriptions be based on NO uptake or the physiological parameter being targeted (Heinonen *et al*., 2000). Martin *et al.* numerically analyzed the variability in uptake efficiency for both delivery modes, with the proportional delivery modelled using a concentration of 20 ppm iNO, and the pulsed flow modelled from an 800 ppm NO/ N_2 source with varying pulse durations and flow rate. Uptake in the lungs for pulsed delivery was found to be dependent on pulse timing, tidal volume, breathing rate, lung and dead space volume, and the lung's diffusive capacity for NO (Martin *et al.*, 2014). These studies all confirm the hypothesis that constant concentration as a dosing metric provides a poor basis for determining the amount of iNO that reaches the patient for

delivery modes where the gas concentration in the patient cannot be constantly monitored. Although compelling arguments have been made for defining dosage in terms of NO uptake from the lungs (Heinonen *et al*., 2000, Martin *et al*., 2014), current research defines pulsed dosage by delivered mass flow rate over time (µg iNO/kg Ideal Body Weight/hour) (Hajian *et al*., 2016, Quinn, D on behalf of Bellerophon Therapeutics, 2019).

Constant flow dosing

Despite older ventilation systems delivering iNO via continuous flow rate many years ago, there are no current dosing metrics particular to continuous flow nor are there models predicting dosage delivery for this mode. Rather, studies involving this mode are outdated and refer to systems that are now no longer in use (Imanaka *et al*., 1997) or use continuous flow as a comparison for the efficacy of other systems and devices (DiBlasi *et al*., 2010, Ivy *et al*., 1998, Kitamukai *et al*., 2002, Westfelt, Lundin, & Stenqvist, 1996). Investigation into noninvasive iNO delivery through a nasal cannula has had positive results for patients with acute right ventricular dysfunction (Tremblay *et al.*, 2019). However, inhaled concentrations and mass flow rates for this delivery method are unknown. Given the advancements in device development for long-term delivery of iNO, including the development of portable devices that don't require large cylinders to deliver the gas, this dosing mechanism warrants further investigation.

1.5 Objectives

To assess noninvasive delivery as a method to administer iNO, this thesis seeks to define dosage delivery using a constant flow rate, and establish these doses in terms of metrics already defined for other delivery modes.

Chapter 2 Study Design Bases

This chapter provides an overview of the literature used to design the study in Chapter 3. In addition to a review of the relevant background literature, adaptations related to the specific work in this thesis are described.

2.1. *In Vitro* Airway Models

The use of *in vitro* airway models in respiratory science can lay the foundation for further *in vivo* research, and can be used to improve clinical implementation, device guidelines and pharmaceutical delivery. In addition, *in vitro* models allow for analysis of delivery parameters that would be otherwise challenging to measure *in vivo*, such as gas composition at the trachea. If airway properties in the bench-top model are carefully selected to be representative of a given patient population, translating experimental data from *in vitro* measurements to predict behaviour of *in vivo* systems can be feasible and effective. For example, the applicability of *in vitro* investigations using airway models has been widely demonstrated in the field of pharmaceutical aerosol delivery (Carrigy *et al*., 2014, Martin, Moore, & Finlay, 2018).

The realistic adult nasal airway model utilized during experimental evaluation in this thesis was developed by Golshahi *et al.* for use in measuring particle deposition in the extrathoracic airways (Golshahi *et al*., 2011). Magnetic resonance images (MRI) of the airways of 10 adults were collected with the approval of the University of Alberta Health Research Ethics Board. The relevant areas (passages from the nares to the trachea) were identified to produce the models (Golshahi *et al*., 2011). Using a rapid prototyping machine, 3D computer models were manufactured from natural colour acrylic plastic.

The nasopharynx and larynx replicas were built separately and attached to the main model later (Golshahi *et al*., 2011). During a study comparing *in vitro* and *in silico* pulsed and continuous flow O_2 delivery, Chen *et al.* evaluated 5 of these models, along with 10 additional airway models produced from high resolution computed tomography (CT) scans using a similar methodology (Chen *et al*., 2017). It was found that intersubject variability across the 15 different models had a coefficient of variation < 5% on the volume-averaged fraction of inhaled oxygen (F_{IO2}) (Chen *et al*., 2017, Chen *et al*., 2019). As such, it was considered reasonable in further work to test on a single representative replica. The replica selected was Subject MRI2 as it had F_{IO2} values closest to the average measured across the 15 replicas (Chen *et al*., 2019), as seen in Figure 2-1. Given that the research undertaken in this thesis measured volume-averaged gas concentrations at the trachea, Subject MRI2 was used as the representative airway following the same reasoning.

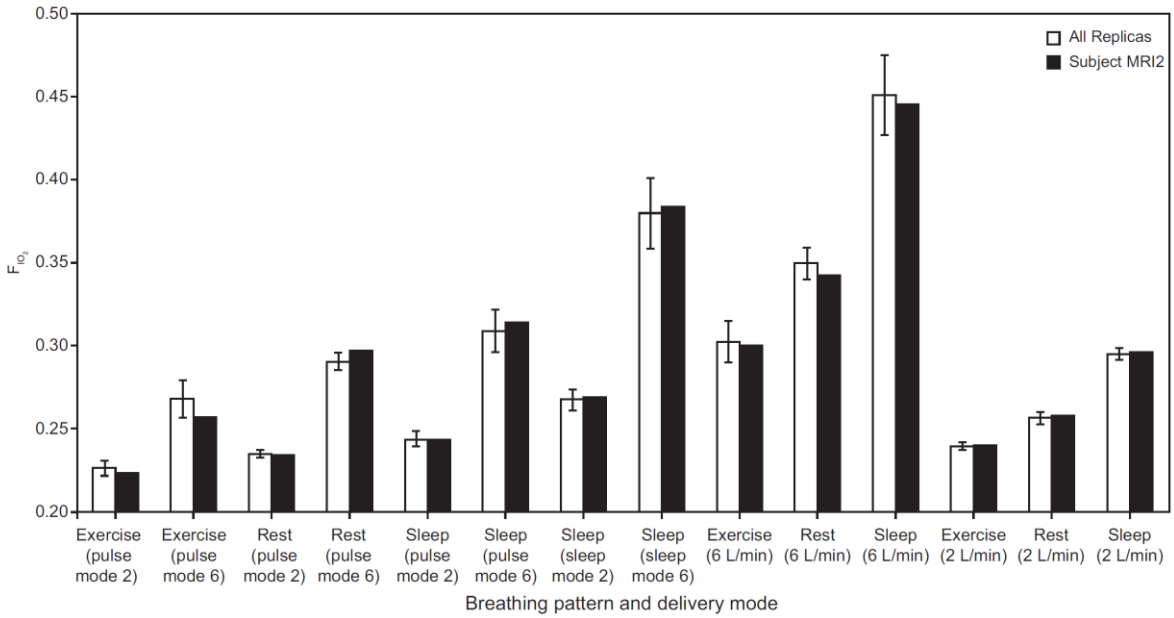

Figure 2-1 Produced by Chen et al., this figure shows the validity of using a single airway replica MRI2 to approximate delivery across 15 subjects. FIO2 for each delivery mode and breathing pattern is compared for an average across all replicas and subject MRI2(Chen et al., 2019).

2.2 Carbon Dioxide as a Surrogate Gas For iNO

During the experimental design outlined for *in vitro* delivery of inhaled NO through nasal cannula at continuous flow rates in Chapter 3, carbon dioxide was used as a surrogate gas to mimic nitric oxide delivery and flow. The FDA considers the use of a tracer gas to simulate nitric oxide flow in device testing to be valid when an adequate response time for NO measurements can not be produced (US Food and Drug Administration, Centre for Devices and Radiological Health, 2000). If transport of NO and CO_2 flow respectively through an airway is dominated by convection rather than the molecular diffusivity of the gases, then CO_2 use is appropriate as a substitution for NO. To assess this, the Peclet number of both gas mixtures was calculated. Peclet number is a dimensionless number that relates convective transport to diffusive transport. It is represented by the following equation:

$$Pe = \frac{convective\ transport}{diffusive\ transport} = \frac{UL_{char}}{D} \quad [2\text{-}1]$$

where U= flow velocity, L_{char} = characteristic length, D = diffusive coefficient. Using the equation for hydraulic diameter, and the airway volume (V) and surface area (SA) for airway replica MRI2 (Chen *et al.*, 2017), the characteristic length was determined using:

$$L_{char} = \frac{4A}{P} \approx \frac{4V}{SA} \quad [2\text{-}2]$$

Constant flow velocity (U) for a standard inhalation flow rate of 10 L/min, along with the molecular diffusivities of NO (0.23 cm^2/s) and CO_2 (0.14 cm^2/s) in air, was applied to equation 2-1. Both Pe numbers were large (Pe>1000), confirming that the flow of gas mixtures containing either NO or CO_2 in the upper airways is dominated by convection, thereby supporting the use of CO_2 as a surrogate gas for NO.

2.2 Data Processing of Gas Samples

During an *in vitro* study measuring pulsed and continuous flow oxygen delivery in realistic adult nasal airway replicas Chen *et al.* proposed a testing protocol to evaluate the volume-averaged F_{IO2} over the course of inspiration (Chen *et al.*, 2017). The continuous flow portion of this study entailed an *in vitro* setup representative of a COPD patient's respiratory physiology and breathing pattern, sampling of the real-time O_2 concentration at the trachea and finally, numerical integration of the O_2 flow rate. During the *in vitro* portion of this investigation, realistic airway replicas were connected to a lung simulator, while O_2 was delivered through a nasal cannula from its source, a portable oxygen concentrator (POC). Oxygen was continuously sampled from the trachea by a gas analyzer and the samples were processed to produce a volume-averaged estimate of F_{IO2} on a breath-by-breath basis (Chen *et al*., 2017). Some of the methodology from this protocol was adapted for the experiments detailed in Chapter 3; however, the approach to measuring carbon dioxide (instead of O_2 from a POC) delivered to the trachea uses different parameters and delivery mechanisms.

Volume-averaged CO_2 concentration for one breath was calculated from multiple real-time tracheal CO_2 samples measured over the course of inspiration. This conversion was adapted from a similar procedure for oxygen described by Chen *et al.* (Chen *et al.*, 2017). The flow rate of carbon dioxide passing through the trachea over time ($\dot{V}_{CO_2}$) was calculated by

$$\dot{V}_{CO_2} = \dot{V}_{inspiration} \times [CO_2]_x \qquad [2\text{-}3]$$

at each time point. $[CO_2]_x$ is the concentration of the gas at time t=x. The inspiratory flow rate ($\dot{V}_{inspiration}$) was imposed and monitored over the breath by the lung simulator (ASL

5000 Breathing Simulator; IngMar Medical, Pittsburgh, PA, USA). $\dot{V}_{inspiration}$ is influenced by tidal volume (V_T), inspiratory time (t_i) and breathing frequency. Tidal volume represents the average volume of gas inhaled during periodic breathing while inspiratory time represents the time taken to inhale in a breath. The start and end of inspiration was determined by the times when the flow rate crossed zero. The CO_2 flow rate was then integrated across inspiration, using the trapezoidal rule, to determine the volume of carbon dioxide inhaled in each breath, ie.

$$V_{CO_2} = \int_{t_0}^{t_n} \dot{V}_{CO_2} \cdot dt = \frac{\Delta t}{2}\left(\dot{V}_{CO_2}(t_0 + t_1)\right) + \frac{\Delta t}{2}\left(\dot{V}_{CO_2}(t_1 + t_2)\right) + \cdots + \frac{\Delta t}{2}\left(\dot{V}_{CO_2}(t_{n-1} + t_n)\right) \quad [2\text{-}4]$$

Tidal volume V_T was similarly calculated from inspiratory flow rates:

$$V_T = \int_{t_0}^{t_n} \dot{V}_{inspiration} \cdot dt = \frac{\Delta t}{2}\left(\dot{V}_{inspiration}(t_0 + t_1)\right) + \cdots + \frac{\Delta t}{2}\left(\dot{V}_{\dot{V}_{inspiration}}(t_{n-1} + t_n)\right) \quad [2\text{-}5]$$

Finally, the volume-averaged concentration of inhaled carbon dioxide in that breath was calculated:

$$[CO_2] = \frac{V_{CO_2}}{V_T} \quad [2\text{-}6]$$

2.3 Gas Sampling Delays

In order to accurately compute and process samples during *in vitro* testing, potential delays and errors in the measurement process should be accounted for. In the case of side-stream gas sampling, there exists an innate delay in measurements of the gas concentration as a result of the time during which the sample gas is being transported

from the sampling site through the sampling tubing to the analyzer (Langer *et al.*, 1985) along with an electronics delay. The aforementioned flow rate and gas concentration signals need to be aligned prior to integration to avoid computational errors (Bernard, 1977). In addition, O_2 and CO_2 analyzers used *in vivo* in gas exchange measurements are known to lack the capacity to provide an immediate step response to a step change in the actual gas concentration. Not accounting for this time response in the analyzer can result in gas exchange being underestimated by a possible factor of 20% (Mitchell, 1979).

Incorporation of the system's time constant into gas sample processing prior to integration accounts for these inherent delays and improves the accuracy of concentration estimates. The natural step response of these analyzers is approximated by a first order exponential function (Mitchell, 1979); as such, the time constant of the system can be easily estimated following the procedure outlined by Langer *et al* (Langer *et al.*, 1985). Using a three-way valve system between the sampling entry port of the analyzer and two gas mixtures of known concentration (X and Y), an approximate step change in gas concentration can be induced by rapidly switching the gas at the sample port from concentration X to concentration Y. For a monoexponential function, the time constant can be assessed be measuring the difference between the time at the start of the step response and the point at which the signal reaches 63% of it's maximum value. In Chapter 3, the time constant utilized during data acquisition is briefly outlined. As the approximation of the system time constant involved calculations following the method discussed by Langer *et al.* it will be discussed here.

A three-way stopcock, depicted in Figure 2-2A, allowed the gas supply to the sampling port of the analyzer (GA-200; iWorx, Dover, NH, USA), which uses infrared to measure CO_2, to be rapidly switched from delivery of O_2 (containing 0% CO_2) to that of 100% CO_2.

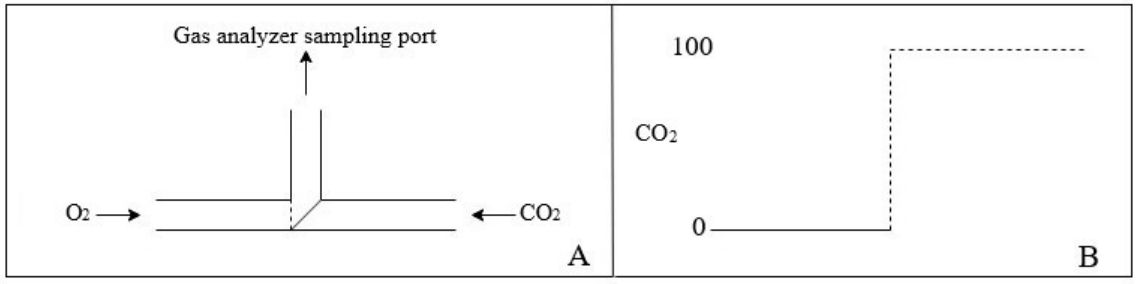

Figure 2-2 Frame A shows the basic mechanic behind the step response. Oxygen supply to the gas analyzer is rapidly switched to carbon dioxide. The switch is represented by the dotted line. Frame B shows the idealized step response of the gas analyzer to this change.

Ideally, a change of this nature would produce a waveform demonstrating a clear step response, as displayed in Figure 2-2B. However, the response from the carbon dioxide analyzer is instead closer to the response shown by the blue (dashed) line in Figure 2-3. The maximum slope for the sampled data was calculated; this was then used to find the y-intercept for a straight line approximation of the analyzer's gradual step response. For the case shown in Figure 2-3, this approximation is represented by:

$$f(x) = 2872t - 1352 \qquad [2\text{-}7]$$

where f(x) is the CO_2 concentration, and t represented the individual time samples recorded from the analyzer.

The time point for 63.2% of the final value (100% CO_2) was then calculated using f(x), along with the time point representing the switch from 0% to 100% CO_2. For a

monoexponential function $g(x) = 100\%(1 - e^{\frac{-t}{\tau}})$, the time constant, τ, is the time taken for the concentration to reach 63.2% from 0% carbon dioxide. In other words:

$$\tau = t_{63.2\%} - t_{0\%} \quad [2\text{-}8]$$

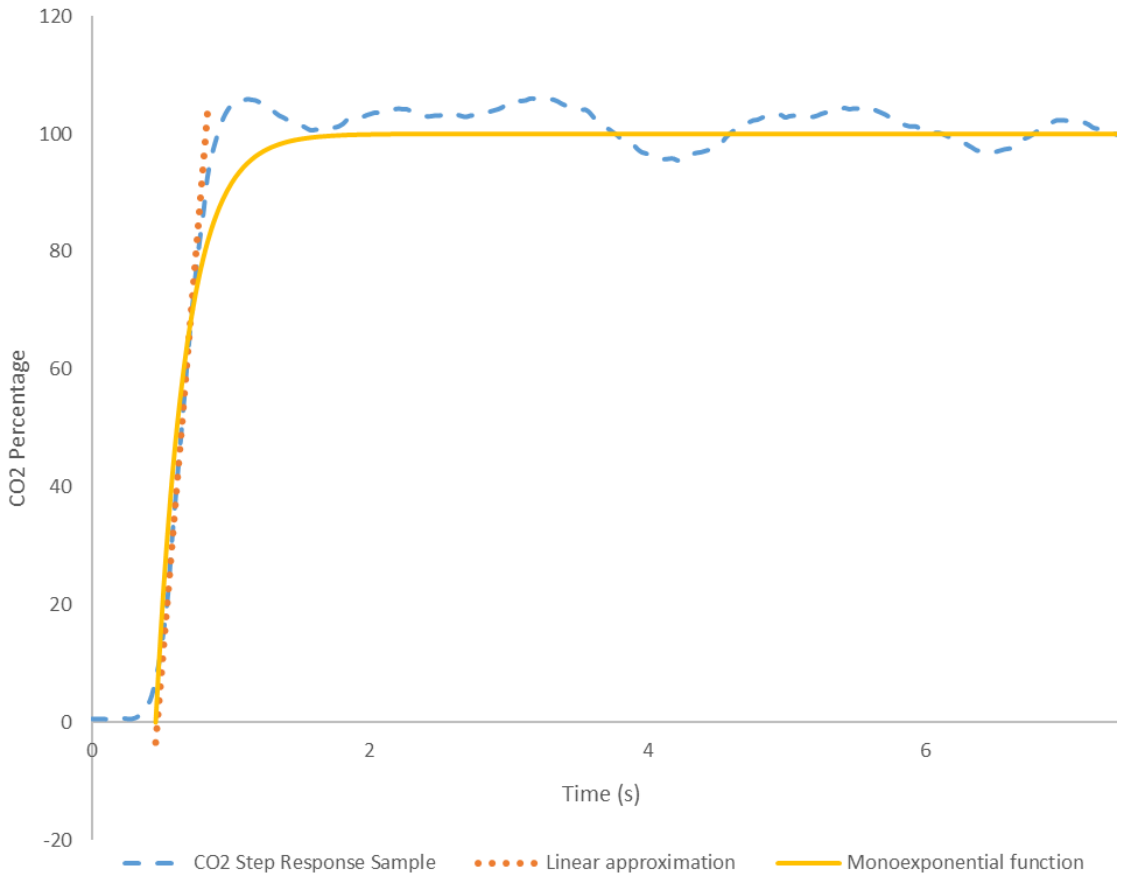

Figure 2-3 The step response for the CO2 analyzer when carbon dioxide is switched from a 0% supply to 100%. The orange (dotted) line represents the linear approximation of the slope. The yellow (solid) represents the monoexponential function approximated using the system time constant.

The time constant was calculated to be 223 ms; it was incorporated into the data processing of CO_2 samples using the following method outlined by Langer et al (Langer et al., 1985) such that the CO_2 concentration at time t=x is represented by

$$[CO_2]_x = \tau \times \frac{([CO_2]_{ox+1} - [CO_2]_{ox})}{\Delta t} + [CO_2]_{ox} \quad [2\text{-}9]$$

where $[CO_2]_{ox+1}$ is the measured CO_2 output from the analyzer at time t_{x+1} and $[CO_2]_{ox}$ is the measured CO_2 output from the analyzer at time t_x. The time constant was applied prior to the step outlined by equation 2-3.

Both f(x) and g(x) provided reasonable approximations for the CO_2 analyzer's step response and are represented by the orange (dotted) and yellow (solid) lines in Figure 2-3.

2.4 Predicting Inspired Gas Concentrations

One of the benefits of benchtop testing lies in the precise control of simulated breathing parameters that tend to vary *in vivo.* The experimental results from *in vitro* tests can be used in a variety of ways to improve clinical outcomes; one of these is through validation of predictive equations. Several studies have proposed dose prediction methodologies and formulae for inhaled oxygen delivered through continuous flow (Duprez *et al*., 2018, Katz *et al*., 2019, Shapiro, Peruzzi, & Kozelowski-Templin, 1994). While there are no studies for continuous flow iNO that do so outside of the present work, the general principles are still applicable and the predictions proposed here will be compared to empirical flow rates and concentrations in Chapter 3. The mechanism for iNO delivered by a continuous flow rate is analogous to continuous flow oxygen therapy. As such, predictive equations proposed for low flow oxygen therapy delivered via nasal cannula could potentially be applied to the present work. To assess the fraction of delivered oxygen during low flow oxygen therapy, Duprez *et al.* evaluated 3 dosage predictive equations against *in vitro* measurements. It was found that delivered oxygen concentrations had the strongest correlation with a prediction formula that accounted for

the patient's respiratory ratio and minute ventilation, as well as the supply flow rate of O_2 (Duprez *et al*., 2018).

Katz *et al*. assessed the dose variability of supplemental oxygen therapy across multiple open patient interfaces, and corroborated these findings. This study assessed the fraction of inhaled oxygen through *in vitro* testing and varied tidal volume, breathing frequency, inspiratory-expiratory ratio and O_2 supply flow rates as well as the patient delivery interfaces (Katz *et al*., 2019). The predictive formulae proposed by Katz *et al.* estimated F_{IO2}, the flow rate of air entering the airways and the inhaled volume of oxygen through inspiratory flow-weighted assumptions. A shared conclusion with Duprez *et al.* was that prediction formulae that do not account for the inspiratory flow rate potentially lead to over- or under-predicting inspired O_2 fractions (Katz *et al.*, 2019). Following the methodology proposed in this study, the inhaled NO concentration at the trachea for a continuous flow rate supplied through a nasal cannula was predicted in the present work using the following equation:

$$[NO]_{predicted} = \frac{Q_{[NO]_{air}} + Q_{[NO]_{supplemental\ O2}} + Q_{[NO]_{supply}}}{Q_{inspiratory}} \quad [2\text{-}9]$$

where $Q_{[NO]_{air}}$ represents the concentration of NO in the entrained room air during inhalation, $Q_{[NO]_{supplemental\ O2}}$ represents the concentration of NO in the supply flow of supplemental oxygen, and $Q_{[NO]_{supply}}$ represents the NO concentration in the NO supply line. $Q_{inspiratory}$ represents the inspiratory flow rate which is calculated by the following equation:

$$Q_{inspiratory} = \frac{V_T}{t_i} \quad [2\text{-}10]$$

where t_i is the inspiratory time.

Neither room air nor 100% O_2 supplied from a gas cylinder contain any NO. As such the flows containing [NO] in the numerator of equation 2-9 can be simplified such that:

$$[NO]_{predicted} = \frac{Q_{[NO]_{supply}}}{Q_{inspiratory}} \quad [2\text{-}11]$$

This simple equation will be applied to the testing in Chapter 3 to assess whether the dose of NO supplied can be reasonably predicted. One of the limitations of the O_2 studies discussed above is that O_2 uptake in the lung was not simulated *in vitro*. As such, the gas concentrations reported would potentially be impacted by the concentration of the gas in the conducting airways not only during inhalation, but also during exhalation. During the experimental design in Chapter 3, iNO absorption in the lungs is simulated, thereby producing more physiologically representative results.

Chapter 3 Inhaled Nitric Oxide: In Vitro Analysis of Continuous Flow Noninvasive Delivery via Nasal Cannula

This chapter has been prepared as a manuscript to be submitted to a scientific journal.

3.1 Introduction

Inhaled nitric oxide (NO) acts as a selective pulmonary vasodilator (Frostell *et al.*, 1991). It is conventionally used to treat persistent pulmonary hypertension in the neonatal population (American Academy of Pediatrics, 2000), and to alleviate pulmonary hypertension in adults and children following cardiac surgery (Checchia, Bronicki, & Goldstein, 2012, Oz and Ardehali, 2004). Use of NO to improve oxygenation in patients with acute lung injury or the acute respiratory distress syndrome has also been studied, though evidence that NO reduces mortality in these patients is lacking (Creagh-Brown, Griffiths, & Evans, 2009, Griffiths and Evans, 2005). The vast majority of patients receiving inhaled NO therapy do so in the intensive care setting, and are simultaneously supported by invasive positive pressure ventilation (Bhatraju *et al*., 2015, Martin *et al*., 2016, Tremblay *et al*., 2019). Modern NO delivery devices adapt the rate at which NO-containing source gas is injected into the ventilator breathing circuit in proportion to the flow of gas in the circuit, so as to maintain a constant NO concentration in the inhaled gas mixture, for example of 20 parts per million (ppm) (Imanaka *et al.*, 1997, Lundin and Stevqvist, 1997, Young, Roberts, & Gale, 1997). As such, dosing recommendations for ventilated patients are currently based on the concentration of NO in the inhaled gas (Griffiths and Evans, 2005, Tworetzky *et al*., 2001), with dose settings typically ranging from ~5 to 80 ppm for marketed NO delivery devices.

In addition to NO administration to ventilated patients, NO administration to ambulatory, spontaneously breathing patients with pulmonary arterial hypertension or pulmonary hypertension secondary to other lung diseases has been investigated, often in combination with long term oxygen therapy (Abman, 2013, Griffiths and Evans, 2005, Quinn, D on behalf of Bellerophon Therapeutics, 2019, Robyn J. Barst *et al*., 2012). These studies have primarily employed devices that deliver NO-containing gas through nasal cannula as a short-duration bolus, or pulse, timed to arrive during the early portion of inhalation. Delivery of gas to the anatomical dead space at the end of inspiration is thereby minimized, in order to conserve NO-containing source gas and extend usage times for small, portable gas cylinders with limited capacity. Such an approach is analogous to pulsed oxygen delivery widely used by oxygen conserving devices (Tiep and Carter, 2008). Pulsed delivery is inherently poorly described using the concentration of NO in the inhaled gas, as the concentration is intentionally varied over each inhalation. Thus, comparison with dosing to ventilated patients at constant NO concentration is challenging. Pulsed delivery has instead been described in terms of the mass of NO delivered per breath (Martin *et al.*, 2014) or per unit time (Hajian *et al.*, 2016).

Additional investigational applications of noninvasive NO delivery to spontaneously breathing patients include delivery through facemasks at high concentration (160 ppm) to cystic fibrosis patients with persistent mycobacterium infection (Yaacoby-Bianu *et al.*, 2018), and delivery through nasal cannula to hemodynamically unstable patients with acute right ventricular (RV) dysfunction (Tremblay *et al*., 2019). Tremblay *et al.* recently reported favourable hemodynamic effects in patients with acute RV dysfunction

receiving noninvasively administered NO. Two-thirds of patients were administered NO in combination with continuous low-flow oxygen through nasal cannula. Although such an approach involves supply of a continuous, rather than pulsed, flow of NO-containing gas, for low-flow nasal cannula the entrainment of room air is variable and depends on patient breathing pattern. Therefore, NO concentration in the inhaled gas mixture is not constant, and comparison with NO dosing done at constant concentration is not trivial.

For an open interface such as a nasal cannula, inhaled NO concentrations are difficult to measure *in vivo* given that mixing of NO-containing gas with entrained room air occurs during transit through the upper airway. In closely related studies of oxygen delivery through nasal cannula, *in vitro* methods incorporating realistic upper airway replicas and simulated breathing have proven useful, allowing variation in inhaled gas concentrations to be analysed throughout the breath (Chen *et al*., 2017, Chen *et al*., 2019, Katz *et al*., 2019). Recently, Katz *et al.* performed *in vitro* experiments to evaluate volume-averaged tracheal oxygen concentrations and volumes of oxygen delivered per minute over a wide range of breathing patterns, patient interfaces, and continuous flow rates. Measured average inhaled oxygen concentrations were accurately predicted using a simple calculation of the flow-weighted average concentration between the delivered oxygen flow and the flow of entrained ambient air. A key variable in predicting the average inhaled oxygen concentration was the average inhalation flow, a function of inhaled tidal volume and inspiratory time. This result echoes the findings of Duprez *et al.* (Duprez *et al.*, 2018), who also recently concluded that the average inspiratory flow has a major impact on average inhaled oxygen concentration during oxygen delivery at low flow to spontaneously breathing patients.

In the present study, we aim to extend these recent *in vitro* results for low-flow oxygen delivery to investigate noninvasive delivery of NO through nasal cannula. Average inhaled NO concentration and inhaled mass of NO over time (referred to here as inhaled NO mass flow) are reported for co-administration of NO with oxygen over a range of cannula types, simulated breathing patterns, and delivered flows. Comparison is made between measured NO concentrations and calculated flow-weighted average concentrations. These results are intended to facilitate an improved comparison between NO delivery at constant flow with established NO dosing at constant concentration, as well as with newer portable devices designed to deliver a target inhaled mass of NO over time.

3.2 Methods

3.2.1 Nasal Airway Replica

The nasal airway replica used in the present study was identical to that used by Chen *et al.* (Chen *et al*., 2019). Selection of this replica was based on the criterion that the volume-averaged fraction of inspired oxygen (FIO2) obtained using the replica was closest to average values obtained in earlier work across a set of 15 replicas (Chen *et al.*, 2017). Furthermore, as it was found that intersubject variability among 15 airway replicas had only a small (5% coefficient of variation) impact on volume-averaged FIO2, use of a single representative replica was deemed reasonable (Chen *et al.*, 2019). As described previously (Chen *et al.*, 2017, Chen *et al.*, 2019), the airway replica used in the present study was built in acrylic plastic using rapid prototyping. It was based on magnetic resonance (MR) images and included airway passages from the nares through

the entrance to the trachea, excluding the oral cavity. The MRI used in the construction of the replica was obtained with University of Alberta Health Research Ethics Board approval (Golshahi *et al.*, 2011). Airway dimensions for the replica were obtained using MeshLab (Visual Computing Laboratory, Istituto di Scienza e Tecnologie dell'Informazione, Italy) and ParaView (Kitware, Clifton Park, NY, USA) (Chen *et al.*, 2017). The selected replica had an interior wall surface area of 287 cm^2 and a total interior volume of 44.6 mL (Chen *et al*., 2017).

3.2.2 Experimental Apparatus

Figure 3-1 displays a schematic of the experimental apparatus employed in the present study. As permitted in FDA Guidance (US Food and Drug Administration, Centre for Devices and Radiological Health, 2000), carbon dioxide (CO_2) was used as a surrogate gas to simulate the delivery of NO. Flows of CO_2 and O_2 (Praxair Canada, Mississauga, ON, Canada) were supplied simultaneously to the nasal airway replica via nasal cannula. The flow of each gas from the cylinder source through the cannula was regulated by separate mass flow controllers calibrated for CO_2 (Alicat MC-2SLPM-D/5M; Alicat Scientific Inc., Tucson, AZ, USA) and for O_2 (Alicat MC-20SLPM-D/5M; Alicat Scientific Inc., Tucson, AZ, USA).

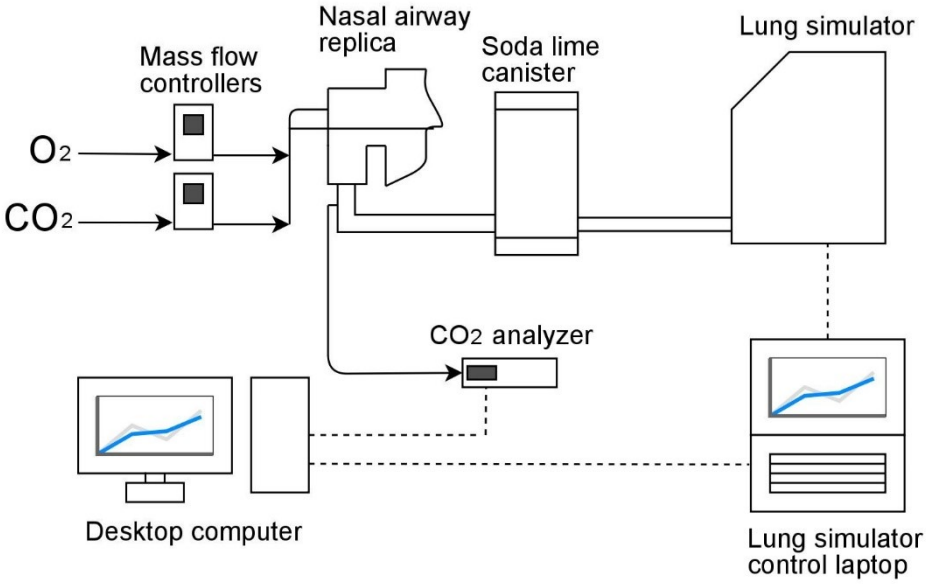

Figure 3-1 Experimental setup used to quantify in vitro performance of inhaled NO delivery through a nasal cannula. Carbon dioxide and oxygen were supplied from cylinder sources, regulated by mass flow controllers and delivered through nasal cannula lumen to an airway replica. The nasal airway replica was connected to a mechanical lung simulator via a canister of soda lime which absorbed the exhaled CO_2. The mechanical lung was programmed with breathing patterns to mimic the breathing of an adult with COPD.

Breathing through the replica was simulated using a programmable lung simulator (ASL 5000 Breathing Simulator; IngMar Medical, Pittsburgh, PA, USA) operated in flow pump mode. The nasal airway replica outlet was connected to a soda lime canister using plastic breathing circuit tubing with 22 mm internal diameter and a total internal volume of 135 cm^3. This volume was selected to be representative of the conducting airway volume from the trachea to the gas-exchange regions of the lungs for an average adult with 3 L functional residual capacity (Finlay, 2001). The canister of soda lime (Spherasorb; Intersurgical, Berkshire, UK) was used to absorb all CO_2 passing through the replica and conducting airway tubing, mimicking an assumed absolute uptake of NO in the gas exchange regions of the lung (Lundin and Stevqvist, 1997, Robyn J. Barst *et al.*, 2012). Preliminary experiments were performed to confirm that use of a 3.6 L canister filled with soda lime was sufficient for absorption of all CO_2 arriving at the canister. The soda

lime was replaced at intervals when a colour change showing saturation in the chemical was noted, or when the CO_2 concentration measured in real-time was too high.

The CO_2 concentration was sampled using a sidestream infrared analyzer (GA-200; iWorx, Dover, NH, USA) at the exit of the airway replica. Data output from the analyzer was processed using data acquisition software (LabVIEW; National Instruments, Austin, TX, USA) that recorded volumetric data from the lung simulator simultaneously.

3.2.3 Breathing Pattern Simulation

Three breathing patterns were selected to provide an approximation of the variability in respiration that an average patient might experience in a day. These patterns mimic the respiratory pattern from a patient at rest, doing light exercise and while asleep, and were based on data from studies done on COPD patients receiving supplemental oxygen (Chatila *et al*., 2004, Hudgel *et al*., 1983). Parameters used to define each breathing pattern are provided in Table 3-1. Inhalation and exhalation cycles both followed a half-sinusoidal shape. The volume of the test lung chamber was logged during breathing at a sampling frequency of 512 Hz using the ASL 5000 software.

Table 3-1 Breathing pattern parameters reproduced in this study. Parameters were selected to reflect an adult subject with COPD.

Breathing Pattern	**Tidal Volume (mL)**	**Inspiratory Time (s)**	**Expiratory Time (s)**	**Breathing Frequency (min^{-1})**	**t_I/t_E**	**t_I/t_{total}**
Rest	640	1.2	2.33	17	0.52	0.34
Exercise	800	0.96	1.77	22	0.54	0.35
Sleep	520	1.79	2.93	13	0.61	0.38

In addition to the breathing patterns defined in Table 3-1, further experiments were conducted at a tidal volume of 520 ml and frequency of 22 min^{-1} as well as at tidal volume of 800 ml and frequency of 13 min^{-1}. Combined with experiments conducted using the rest, exercise, and sleep patterns, these measurements allowed the influence of tidal volume and frequency to be assessed independently, with all other parameter held constant.

3.2.4 Nasal Cannula Types

To investigate any potential differences in gas delivery across different cannula types, three cannulas were used (shown schematically in Figure 3-2):

a) a single lumen (1103; Hudson RCI, Teleflex Medical, Research Triangle Park, NC, USA) where flows of O_2 and CO_2 were pre-mixed using a Y-connector positioned upstream from the cannula,

b) a dual lumen with a different gas going into each nostril (4807-7-7; Salter Labs, Carlsbad, CA, USA)

c) a dual lumen with the gases separated until entering the nares (1165011; Intersurgical, Berkshire, UK).

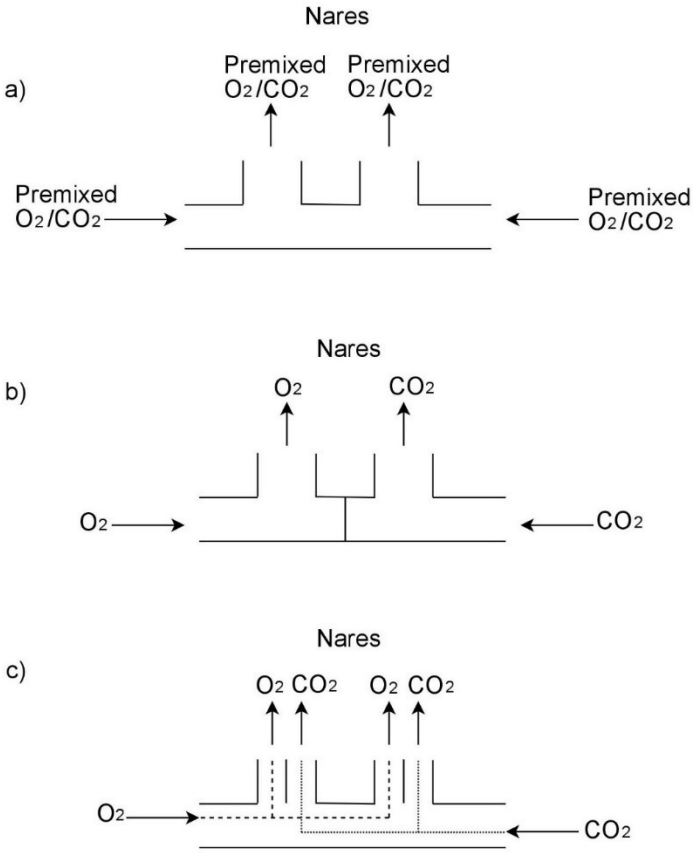

Figure 3-2 Cannula types utilized in experiments: a) single lumen with premixed gases upstream, b) dual lumen with different gases supplied to each nostril and c) dual lumen with both gases (while separated) supplied to each nostril

3.2.5 Gas Flow Rates and Concentration Measurements

As noted above, CO_2 was used as a surrogate gas to simulate the delivery of nitric oxide. In order to prescribe flows of CO_2 for the experimental protocol, corresponding flows of source NO-containing gas were first defined. Continuous NO flows were selected to target average concentrations of 20 ppm and 5 ppm NO at the trachea for the resting breathing pattern. These flows were calculated using the following expression, based on an assumption of complete mixing of the NO flow within the inspired breath (Katz *et al*., 2019):

$$Q_{NO} = \frac{V_T}{t_i} \times \frac{FtNO}{800\text{ppm}} \qquad [3\text{-}1]$$

where Q_{NO} is the supplied NO flow, V_T is the tidal volume, t_i is the inspiratory time, FtNO is the targeted average NO concentration at the trachea (in ppm), and the concentration of NO in the source gas is assumed to be 800 ppm.

Flows of 0.8 and 0.2 L/min of 800 ppm NO were calculated using equation 3-1 to target average concentration of 20 and 5 ppm, respectively, for the resting breathing pattern. Flows of CO_2 supplied in the experiments were set equal to these values, with 100% CO_2 representing 800 ppm NO. CO_2 concentrations were sampled at the exit of the replica (i.e. the trachea), and were corrected for sampling delay and time constant. The CO_2 concentration was sampled at a flow rate of 200 mL/min, which is two orders of magnitude smaller than average inhalation flows and as such is not expected to have any appreciable influence on flow through the replica and lung simulator. To determine the time constant of the sampling system, preliminary experiments were conducted in which the gas supply to the analyzer was rapidly switched via a three-way stopcock between two different gas mixtures of known concentration (0% and 100% CO_2). A time constant of 223 ms was calculated based on the time taken for the system's response to reach 63% of its final value following this step change in the input concentration. Correction to the CO_2 concentration recorded over time was then done under the assumption of a first order system following methods described in Langer *et al.* (Langer *et al*., 1985) and adopted previously by Chen *et al*. (Chen *et al*., 2017). The volumetric flow of carbon dioxide passing the trachea was then determined by multiplying the known inspiratory flow with carbon dioxide concentration. The trapezoidal rule was used to integrate the carbon dioxide flow over each inhalation to determine the volume of carbon dioxide inhaled per breath. After following a similar procedure to determine the measured tidal volume, a volume-averaged value for the concentration of carbon dioxide per breath was found by

dividing the volume of CO_2 by V_T. Using a conversion factor of 100% CO_2 = 800 ppm NO, the corresponding inhaled NO concentration was then calculated. Results reported below are presented in terms of these corresponding NO values. All measurements were conducted approximately 60 breathing cycles after supply gas flows were started, which allowed the system to reach steady state as confirmed by observing real-time gas concentration waveforms.

Experimental NO concentrations were compared to predicted concentrations. Predicted values were calculated using:

$$[NO]_{predicted} = \frac{Q_{NO} \times 800\ ppm}{\frac{V_T}{t_i}} \quad [3\text{-}2]$$

Mass flow rate past the trachea was calculated from the following equation:

$$Mass\ flow\ rate = [NO]_{trachea} \times V_T \times breathing\ frequency \times \rho_{NO} \quad [3\text{-}3]$$

where ρ_{NO} = 1.34 kg/m^3 at 20^{o}C and 1 atm

Efficiency of delivery (η) to the trachea was evaluated by the formula:

$$\eta = \frac{Measured\ NO\ mass\ flow\ rate}{Supplied\ NO\ mass\ flow\ rate} \quad [3\text{-}4]$$

3.2.6 Experimental Design

Experiments were conducted with flows of 0.2 L/min and 0.8 L/min CO_2 and a supplementary O_2 flow of 2 L/min. Three breathing patterns (sleep, rest and exercise) were used and tests were run with all three cannulas. Following this, additional

experiments were conducted using only one cannula (Intersurgical) across the three breathing patterns and both carbon dioxide flow rates, but at an oxygen flow of 6 L/min.

A final set of experiments was performed to independently vary tidal volume and breathing frequency. Using one nasal cannula (Intersurgical), the breathing frequency for the sleep and exercise breathing patterns were exchanged while maintaining the original tidal volumes.

For each experimental condition, three replicate tests were executed and for each replicate the inhaled NO concentration was determined as the average of 5 consecutive breaths. Measurement uncertainty for $[NO]_{trachea}$ reported below is estimated as one standard deviation across replicate tests. Uncertainty for $\dot{m}_{NO}$ and η was calculated by propagating error using standard error analysis techniques(Taylor, 1997).Variability between average nitric oxide concentrations obtained on separate days, and from different points on the circumference of the trachea base, were found to be of similar magnitude as the variation between individual breaths.

3.2.7 Statistical Analysis

Multiple 2-factor ANOVA tests were performed to compare the influences of cannula and breathing pattern on average NO concentration and NO mass flow. Two separate ANOVA tests were executed for each flow (0.2 L/min and 0.8 L/min of 800 ppm NO supply). A significance level of alpha = 0.05 was used. Tukey post-hoc analyses were performed. Unpaired two-tailed student's T-tests were also performed to assess the impact of varying supplemental oxygen flow rates on NO concentration. Additional unpaired two-tailed student's T-test were conducted to compare relative influences of NO

flow on efficiency. Post-hoc analyses were performed using the VassarStats online tool (VassarStats, Vassar College, NY, USA) with the remainder of the statistical analysis performed in the Excel environment (Microsoft, Redmond, WA, USA).

3.3 Results

Tracheal NO concentration waveforms displayed a consistent shape across all parameters studied, as exemplified in Figure 3-3. The shape of the waveform can be explained as follows (Chen *et al*., 2017):

1. The first, taller peak indicates pooling in the airways at the end of expiration. Since NO flow is supplied continuously throughout the breath, it will accumulate in the upper airways as exhalation ends and the expiratory flow rate approaches zero. This pooled NO is then inhaled at the start of the next inspiration, which is reflected in the sharp peak in concentration.

2. Once the pooled NO is inhaled, the inspiration flow then increases toward a maximum, so correspondingly the fraction of inhaled gas represented by NO decreases, which is reflected in a steep decline in NO concentration. Conversely, as the inspiration flow passes its peak and begins to decrease again, the NO fraction in the inhaled gas increases.

3. As exhalation begins, gas remaining in the dead space between the airway replica and test lung is first to be exhaled. The NO concentration decreases as the dead space gas is exhaled.

4. As exhalation proceeds, the NO concentration approaches zero, reflecting complete absorption in the simulated peripheral lung region.

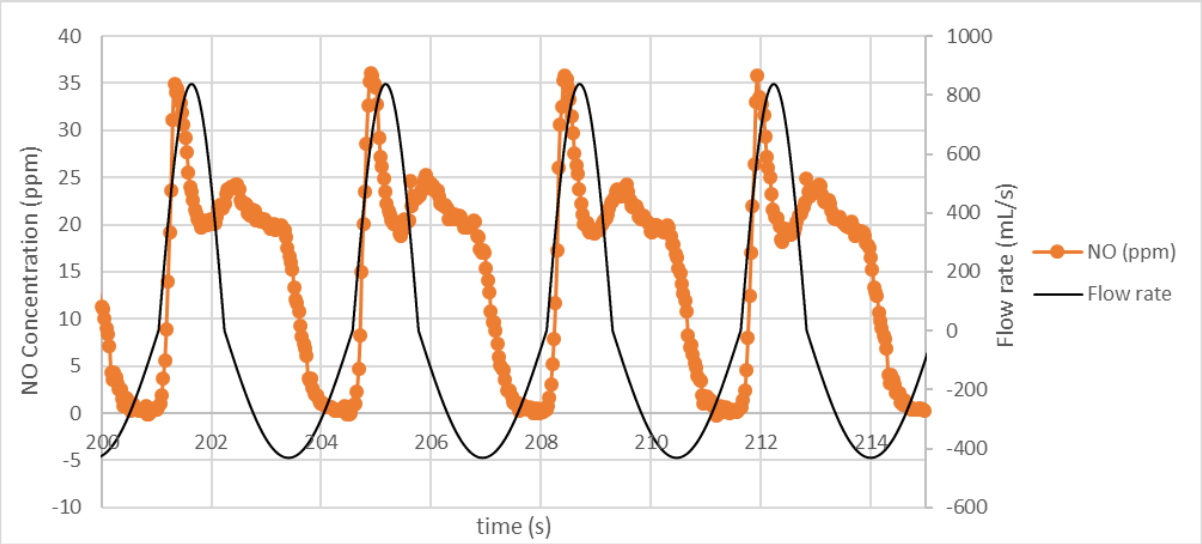

Figure 3-3 Sample NO concentration and total flow rate past the trachea recorded during data acquisition process for 0.8 L/min of 800 ppm NO supply at rest with 2 L/min supplemental O_2. NO concentration drops towards zero at the end of each breath as NO that is not absorbed is exhaled.

3.3.1 NO Concentration

Volume-averaged tracheal NO concentrations were found to be highest for the sleep breathing pattern and lowest for exercise. Figures 3-4 and 3-5 show the average NO concentrations during inhalation for varied NO and O_2 supply flows. Influences of cannula type and breathing pattern were statistically significant ($p<0.001$). Post-hoc analysis confirmed the consistent significance of breathing pattern across all pairs of data ($p<0.01$). While influence of cannula type was statistically significant, differences observed between cannula types were small in comparison to differences observed between breathing patterns. When averaged over the three cannula types, average inhaled tracheal NO concentrations were 23.3±0.5 ppm, 36.5±1.4 ppm, and 17.2±0.3 ppm, for the rest, sleep, and light exercise breathing patterns, respectively, for the case of a target NO concentration of 20 ppm at rest (Figure 3-4).

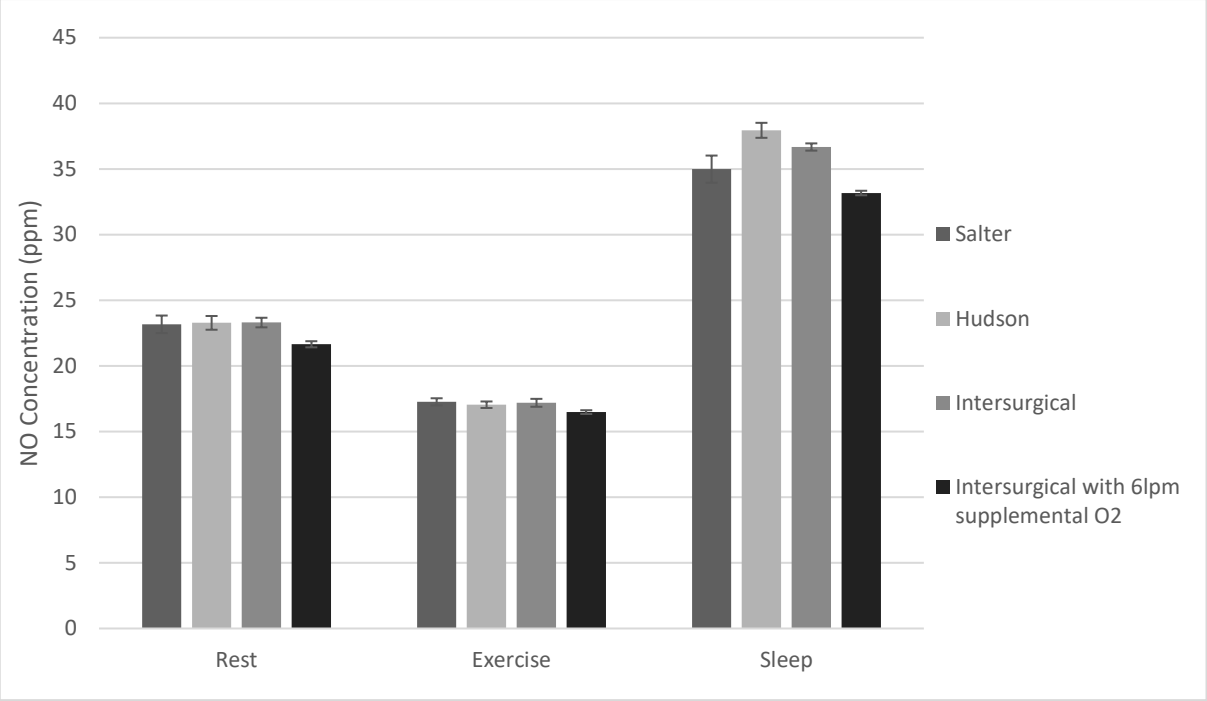

Figure 3-4 Average inhaled NO concentration at the trachea for 0.8 L/min of 800 ppm NO supply, presented by breathing pattern. The grey columns each represent average tracheal NO concentration for 2 L/min supplemental O_2 with different cannulas while the black column represents the concentration for 6 L/min supplemental O_2 with an Intersurgical cannula.

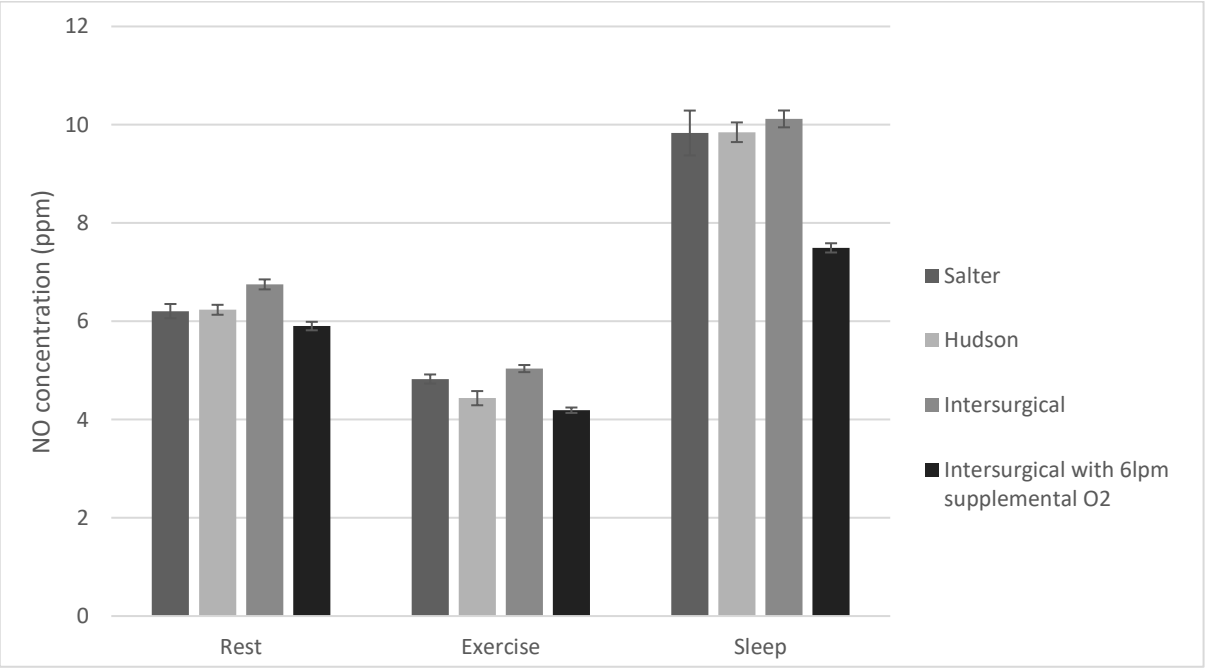

Figure 3-5 Average inhaled NO concentration at the trachea for 0.2 L/min of 800 ppm NO supply, presented by breathing pattern. The grey columns each represent average tracheal NO concentration for 2 L/min supplemental O_2 with different cannulas while the black column represents the concentration for 6 L/min supplemental O_2 with an Intersurgical cannula.

In five of six cases, differences between average inhaled tracheal NO concentration for the 2 versus 6 L/min oxygen flow were statistically significant ($p<0.05$). Supplying a higher oxygen flow resulted in lower NO concentrations; however, these effects were again small in comparison to differences observed between breathing patterns (Figures 4 and 5).

Average inhaled tracheal NO concentrations were slightly higher than those predicted using Equation 3-2, with the greatest deviation in delivery being for the exercise breathing pattern and the closest agreement to the prediction being for the sleep pattern, as can be seen in Figure 3-6. In all cases, inhaled tracheal NO concentrations were predicted within ± 4.5 ppm

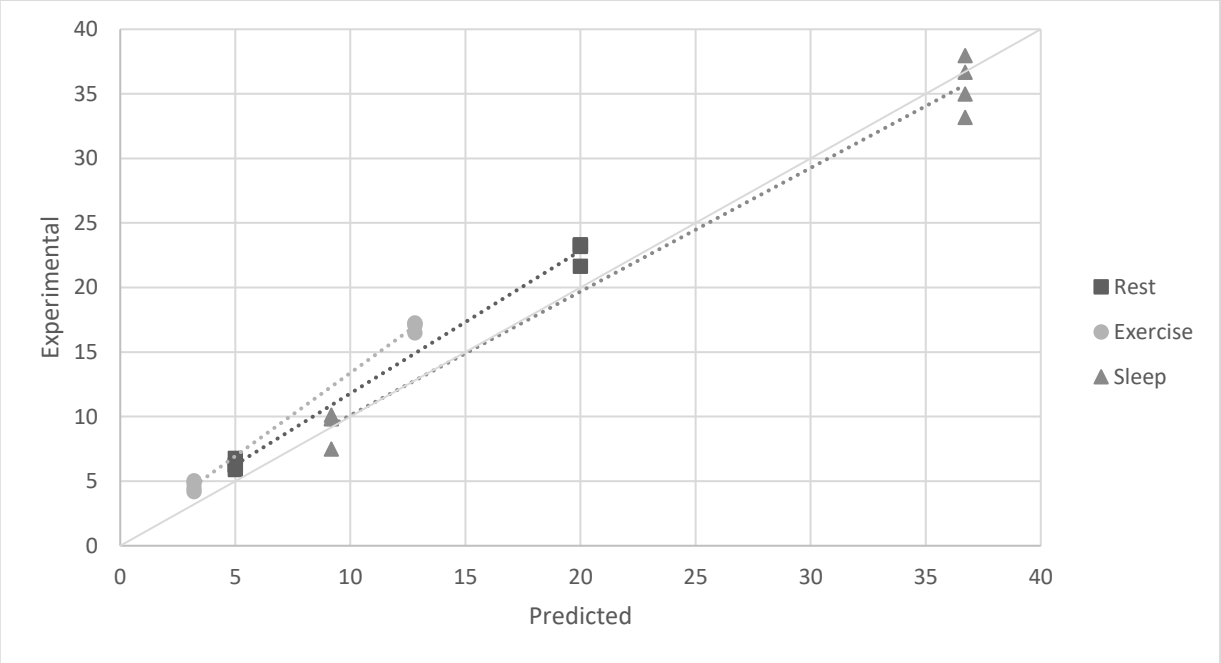

Figure 3-6 Differences between the experimental and predicted NO concentrations at the trachea, separated by breathing pattern. Measured NO concentration was best predicted for the sleep breathing pattern while rest and exercise were progressively poorly predicted. Sleep had the highest concentrations while exercise had the lowest.

3.3.2 Mass Flow Rate Past the Trachea

Inhaled NO mass flow was highest for the exercise breathing pattern and comparable between sleep and rest patterns. Figures 3-7 and 3-8 show inhaled NO mass flow for varied NO and O_2 supply flows, and for different breathing patterns. The influences of breathing pattern ($p<0.001$) and cannula type ($p<0.05$) were both statistically significant. Differences observed between cannula types were small in comparison to differences observed between breathing patterns. Post-hoc analysis confirmed the significance of breathing pattern between sleep and exercise, and between rest and exercise ($p<0.05$). Between rest and sleep, 3 out of 6 results showed significance; however, relative differences in NO mass flow across breathing patterns were much smaller than those in NO concentration. At the higher supply flow (Figure 3-7), when averaged over the three cannula types, mass flow rate of NO past the trachea was 20.3±0.5 mg/hr, 19.9±0.8 mg/hr, and 24.3±0.4 mg/hr for the rest, sleep, and light exercise breathing patterns, respectively.

In five of six cases, differences between inhaled NO mass flow for the 2 versus 6 L/min oxygen flow were statistically significant ($p<0.05$). Supplying a higher oxygen flow resulted in lower NO mass flow at the trachea.

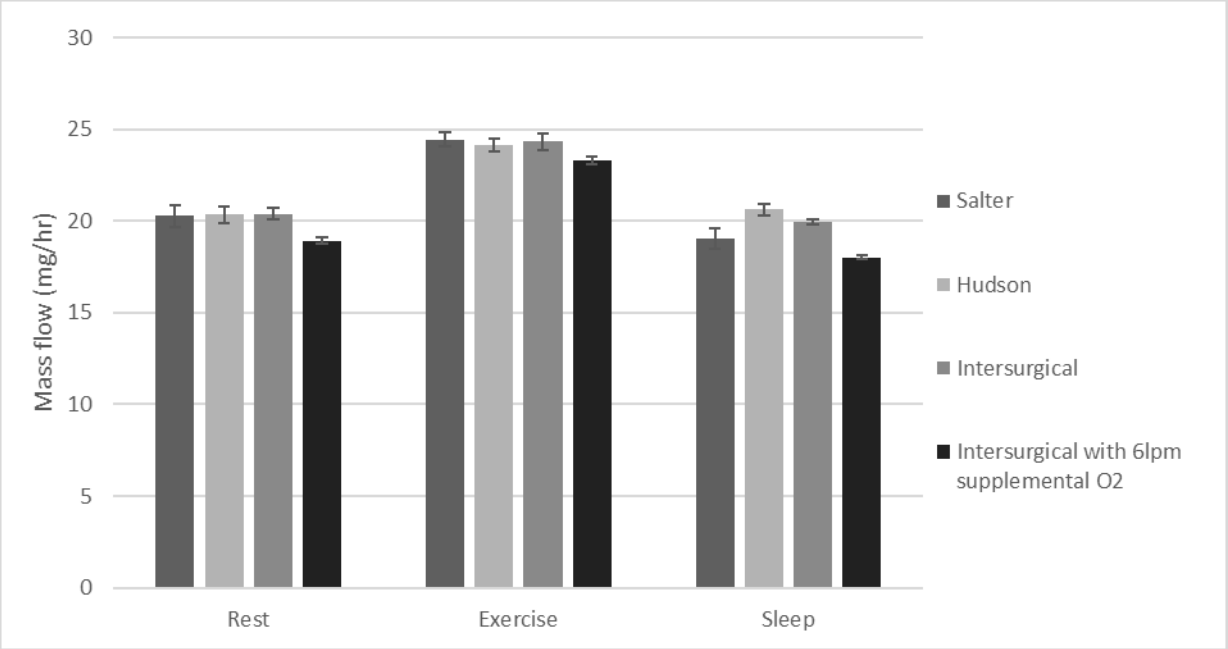

Figure 3-7 Mass flow rate per breath past the trachea for 0.8 L/min of 800 ppm NO supply, presented by breathing pattern. The grey columns each represent average mass flow rate for 2 L/min supplemental O_2 with different cannulas while the black column represents the mass flow rate for 6 L/min supplemental O_2 with an Intersurgical cannula.

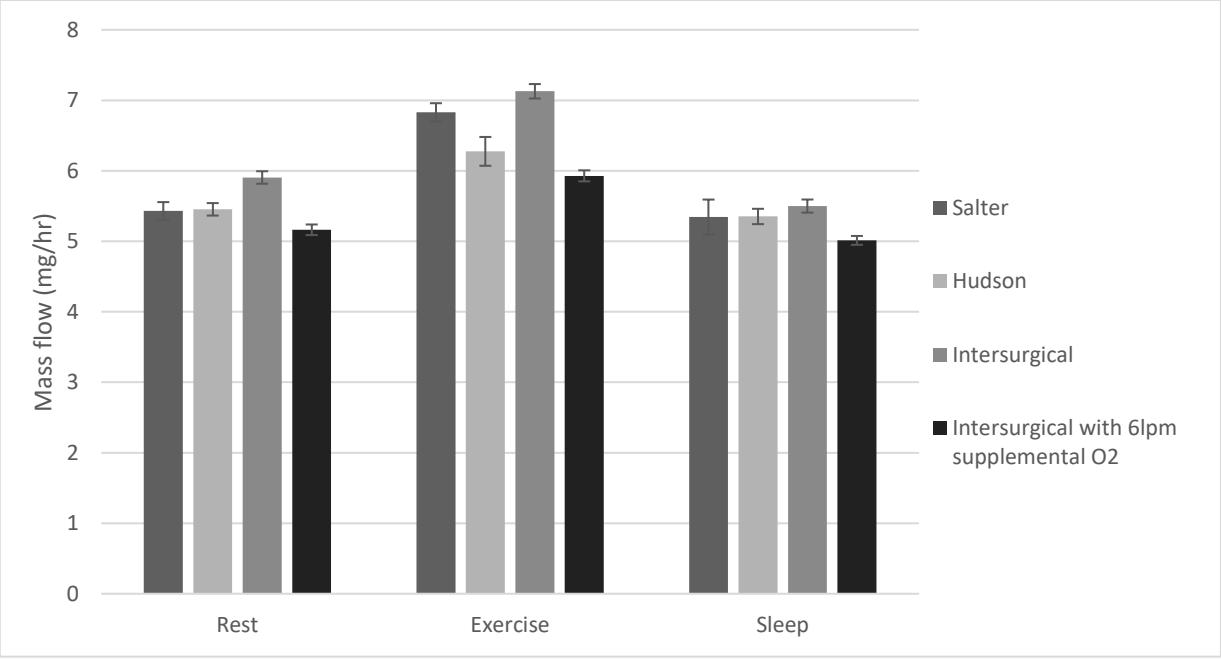

Figure 3-8 Mass flow rate per breath past the trachea for 0.2 L/min of 800 ppm NO supply, presented by breathing pattern. The grey columns each represent average mass flow rate for 2 L/min supplemental O_2 with different cannulas while the black column represents the mass flow rate for 6 L/min supplemental O_2 with an Intersurgical cannula.

3.3.3 Delivery Efficiency

Delivery efficiency showed a dependency on both breathing pattern and supply flow rate. Seven out of nine t-tests comparing efficiencies at high and low NO supply flows were statistically significant ($p < 0.05$). The delivery efficiencies at the high NO supply flow averaged between 37 to 47%, while efficiencies at the low NO supply rate averaged between 40 to 53%. For both high and low NO supply flows, the exercise pattern showed the highest delivery efficiency while sleep and rest were comparable.

In order to evaluate whether this difference could be attributed to variation in tidal volume versus breathing frequency, additional experiments were conducted to vary these two parameters independently. When the breathing frequency was decreased from 22 to 13 min^{-1} for the high NO supply flow with V_T = 800 mL, mass flow dropped by 4 mg/hr and the efficiency dropped by 8%. Conversely, when the breathing frequency was increased from 13 to 22 min^{-1} for the high NO supply flow with V_T = 520 mL, mass flow increased by 2 mg/hr and the efficiency increased by about 5%. For patterns with the same breathing frequency at the high supply flow, when V_T was decreased from 800 mL to 520 mL at breathing frequency = 22 min^{-1}, the mass flow rate dropped by 2 mg/hr and the efficiency dropped by 4%. Conversely, when V_T was increased from 520 mL to 800 mL at breathing frequency = 13 min^{-1}, the mass flow rate increased by only 0.5 mg/hr and the efficiency increased by 1%.

3.4 Discussion

The present study provides measurement of the NO dose delivered at continuous flow through a nasal cannula across a range of supply flows, breathing patterns and cannula

types. Delivery parameters in the present work were selected to reflect emerging clinical applications, and results were presented across different dose metrics, including NO concentration, which is currently used in the critical care setting, and NO mass flow, which is under investigation for long-term NO administration. Average inhaled NO concentrations measured at the trachea were reasonably well-predicted using a flow-weighted calculation to account for dilution of delivered NO by entrained ambient air. Variability in the inhaled NO dose with breathing pattern was much greater when assessed as an average inhaled concentration, versus a mass flow over time.

Delivery of NO in combination with continuous flow O_2 was assessed for three different nasal cannula designs. As shown schematically in Figure 3-2, for the single lumen Hudson cannula, flows of O_2 and CO_2 (used as a surrogate for NO) were combined using a Y-connector positioned upstream from the cannula, whereas for the two dual lumen designs (Salter and Intersurgical) CO_2 and O_2 were supplied via individual lumen. Differences in inhaled NO concentration and mass flow between cannula types were small in all cases studied, and not considered to be clinically significant (Figures 3-4, 3-5, 3-7, and 3-8). These data suggest that that mixing of the two supplied gas streams with entrained air within the nasal airways was efficient, such that no advantage or disadvantage was observed when comparing against the pre-mixed, single lumen case. Nevertheless, use of a dual lumen cannula may confer other advantages: it is notable that using a dual lumen interface that keeps NO and O_2 flows separate up to entering the nasal airways would decrease production of nitrogen dioxide (NO_2), a potentially harmful by-product formed by reaction of NO and O_2. Of the two dual lumen cannulas investigated here, only the Intersurgical cannula delivered both NO and O_2 to each nostril, which could be advantageous in circumstances where one nostril is congested or occluded. For these reasons, a dual lumen cannula that delivers NO and O_2 to each nostril (such as the

Intersurgical cannula evaluated in the present experiments) is recommended for continuous flow delivery of NO in combination with supplemental O_2.

The feasibility of noninvasive, continuous flow administration of NO via nasal cannula has recently been demonstrated by Tremblay *et al.* in hemodynamically unstable patients with acute right ventricular (RV) dysfunction (Tremblay *et al.*, 2019). Two-thirds of patients were administered NO in combination with continuous low-flow oxygen, at a median flow of 2 L/min, through nasal cannula. Noninvasively administered NO was associated with favourable hemodynamic effects in these patients, and circumvented the hemodynamically deleterious effects of tracheal intubation (Tremblay *et al.*, 2019). Tremblay *et al.* report delivery of NO at concentrations between 20 and 40 ppm, presumably the concentration of NO in gas delivered to the cannula, prior to dilution by entrained room air. As the present work indicates, average inhaled NO concentrations at the trachea would be considerably lower, and vary with patient breathing pattern. Given the current need for additional prospective studies to evaluate the dose-dependent response to noninvasive nasal NO (Ghadimi and Rajagopal, 2019), accurate predictions of average inhaled NO concentrations are critical. In a previous *in vitro* study assessing NO delivery across multiple delivery interfaces, DiBlasi *et al.* demonstrated the challenge of predicting delivery through an open interface (DiBlasi *et al.*, 2015). In the present study, the average inhaled tracheal NO concentration for a constant flow of fixed concentration showed wide variation across both breathing pattern and supply flow rate. The sleep breathing pattern, which produced low minute volumes, resulted in an average tracheal NO concentration (36.5 ppm at higher NO supply flow, 9.9 ppm at lower NO supply flow) more than double that of the exercise breathing pattern (17.2 ppm at higher flow, 4.8 ppm at lower flow). This indicates that the tracheal concentration of the

delivered gas is strongly influenced by breathing pattern, a result corroborated by similar studies of continuous flow oxygen delivery (Duprez *et al*., 2018, Katz *et al.*, 2019). Reasonably predictive estimates for the average inhaled concentration at the trachea (±4.5 ppm NO at higher flow, ±1.8 ppm NO at lower flow) were obtained in the present work by accounting for the concentration and flow of the source-gas, as well as tidal volume and inspiratory time of the patient (Equation 3-2). Measured concentrations tended to be somewhat higher than predicted, except in the sleep case. This is likely due to pooling of NO-containing gas in the upper airway near the end of expiration, which is not accounted for in the predictive calculation.

Unlike NO concentration, NO mass flow past the trachea was highest for the exercise case and lowest for the sleep and rest cases. Mass flow past the trachea averaged at 21.5 mg/hr for the higher NO supply flow and at 5.9 mg/hr for the lower supply flow. The mass flow for the lower NO supply is comparable with the 75 μg NO/kg IBW/hr dose that was investigated in the INOvation-1 study of pulsed iNO for treatment of PAH (Quinn, D on behalf of Bellerophon Therapeutics, 2019). For example, a patient with 75 kg IBW would receive 5.625 mg/hr, a dose similar to the mass flow reported in the present work. In the present study, it is noted that for both NO supply flows, the range of mass flow results was small across breathing pattern, with results between the exercise case and the other two breathing patterns within a range of ±5.4 mg/hr for the high flow and ±1.6 mg/hr for the low flow. This supports the use of mass flow rate as a dose metric for noninvasive nasal NO administration, as it suggests that, unlike NO concentration, for a fixed supply flow rate the mass flow rate at the trachea can be reasonably estimated without knowledge of the patient's specific breathing pattern.

Delivery efficiency, defined as the ratio of NO mass flow past the trachea to NO mass flow delivered through the cannula, showed a dependency on both breathing pattern and NO supply flow. For both NO supply flows, the exercise pattern had the highest delivery efficiency while sleep and rest had comparable delivery efficiencies. In addition, lower NO supply flows had higher delivery efficiencies. Across all cases studied, measured delivery efficiencies range between 37-53%, whereas the portion of the breath spent in inhalation ranged between 34-38% for the breathing patterns studied. This provides further evidence that some fraction of gas supplied during exhalation pools in the nasal airways, and remains in the airways to be inhaled upon the next inhalation cycle. Inhalation of gas which pooled in the nasal airway during exhalation is thought to explain the initial spike in tracheal gas concentration observed near the start of each inhalation in Figure 3-3.

A limitation of the current work is that NO_2 production could not be measured *in vitro*, since CO_2 was used as a surrogate gas to represent NO. However, using the methodology outlined by Tsukahara *et al.* an estimate of NO_2 formed during the mixing of NO and O_2 in the single lumen cannula (Hudson RCI) was calculated (Tsukahara, Ishida, & Mayumi, 1999). The maximum NO_2 produced was 0.49 ppm and represents 0.21% of the NO concentration in the flow, confirming that even for a single lumen continuous low flow system there would likely be insufficient residence time in the lumen tubing for significant concentrations of NO_2 to form. In addition, the NO flow is further diluted a minimum of 6 times during the mixing of cannula gases and entrained room air. These inconsequential resulting concentrations negate the necessity for measuring NO_2 in the present work.

3.5 Conclusion

Nasal cannula type had minimal effect on noninvasive continuous flow NO delivery, while breathing pattern and supply flow strongly influenced average inhaled NO concentrations monitored at the trachea. Delivery efficiency was higher at lower supply flow rates, and for breathing patterns that had a high minute volume. While average inhaled NO concentrations were reasonably well predicted with flow-weighted calculations; there was a wide variation in inhaled concentration over different breathing patterns. Inhaled mass flow of NO provides a more consistent dosing metric for noninvasive continuous flow NO, as variation across breathing patterns was small.

Chapter 4 Conclusions and Recommendations

4.1 Summary

This thesis aimed to provide a basis for dosage estimation of inhaled nitric oxide delivered by a constant flow rate through a nasal cannula. Inhaled nitric oxide (iNO) is used as a selective pulmonary vasodilator to alleviate pulmonary hypertension and improve oxygenation in critically ill patients. It is currently delivered primarily through invasive mechanical ventilation; however, there has been investigation into ambulatory administration through noninvasive means. The characterization of dosage delivery provided in this thesis provides a delivery basis for iNO supplied through a nasal cannula. In addition, the close correlation between predicted and measured dose delivery confirms that, similar to F_{IO2} for oxygen (Katz *et al.*, 2019), delivered iNO concentration is strongly influenced by the inspiratory flow rate of the patient.

Delivered NO was presented across two different metrics, tracheal NO concentration and iNO mass flow rate past the trachea. Constant concentration is the dosing metric currently used for mechanical ventilation while iNO mass flow rate is used for pulsed flow systems that are under investigation. Presenting delivery across both provided a basis for dosage estimation in terms of both strategies. Delivery was modelled by supplying carbon dioxide (representing iNO through the ratio 1% CO_2 = 8 ppm NO) and supplemental O_2 through a nasal cannula to an adult airway replica, which was in turn connected to a mechanical lung simulator. Three breathing patterns were compared for variation in delivery during a patient's different activities throughout the day, followed by a variation in breathing frequency for a fixed tidal volume to determine which factor impacted delivery. Three different cannulas with varying mixing strategies were tested to

determine how delivery was affected by cannula design. In addition, delivery was compared for two supply flow rates of NO (0.2 and 0.8 L/min) and two oxygen flow rates (2 and 6 L/min). Tracheal NO concentrations were found to be influenced largely by supply flow rates and breathing patterns while cannula selection influence was negligible. An increase in overall minute volume resulted in larger discrepancies between predicted and experimental concentrations. On the other hand, iNO mass flow rate past the trachea was found to be influenced far less than concentration by variation in breathing pattern, with similar delivery during rest and sleep and moderately higher delivery during exercise. Although the proposed predictive equations proved to be reasonably accurate, the high variation in tracheal NO concentration across breathing pattern suggests that dose prediction will prove challenging since the patients breathing parameters would need to be known, which would be difficult during ambulatory administration. Conversely, the small range in mass flow delivery across breathing patterns bodes well for its use as a dosing metric as dose delivery could be reasonably well predicted across a range of activity for a given patient.

Although pulsed flow delivery has been investigated as the next step for iNO administration, the current work suggests that constant flow delivery is a feasible delivery system and warrants further investigation. Unlike pulsed flow, constant flow delivery is an inherently simple technique. Source iNO-containing gas is supplied with supplemental oxygen via a nasal cannula. It mixes with entrained room air as it travels through the upper airway. As such, the resulting concentration of iNO in the inhaled gas that reaches the conducting airways is variable due to the multitude of factors: inspiratory time, tidal volume of the patient, flow rate of iNO-containing gas and the concentration of source iNO-containing gas. The mass flow rate of iNO, however, can be reasonably predicted

within a range and delivers doses well within the safe range for clinical applications. Indeed, many of the arguments in favour of pulsed flow delivery apply to continuous noninvasive delivery too. As technology has advanced, so too have devices for ambulatory administration of iNO: some of the portable devices under development for iNO do not require a separate, stationary cylinder source to supply NO into the inspiratory portion of the delivery interface. Instead, these devices provide iNO through mini cylinders (Hajian *et al*., 2016) or synthesize it from the air (Zapol and Yu, 2016). However, these devices are intended for pulsed flow delivery and as such are not yet commercially available.

For a well-ventilated space (10-12 air changes/hour), it is unlikely that the surrounding environment will be contaminated with NO for delivery at low flow rates (Cuthbertson, B. H. *et al*., 1997). However, a concern has been raised that iNO inhaled over a long period could cause a decrease in oxygenation in people with lung injuries (Barbera and Roca, 1996). However, there are studies that report otherwise (Germann *et al*., 1998, Lundin, S. *et al*., 1999), suggesting that the conditions under which resulting oxygenation is poor may be specific to particular clinical conditions rather than a generalized result. Regardless, while constant flow delivery may not be appropriate for all applications of iNO therapy, the results presented in this thesis have positive implications for the feasibility of this delivery method.

4.2 Future Work

In this study, experiments were performed to measure the tracheal NO concentration and mass flow rate for constant flow of iNO through a nasal cannula. While reasonable agreement was observed between predicted and measured tracheal iNO concentrations,

further experiments exploring a broader parameter range, particularly in breathing frequency, might better elucidate reasons for discrepancies between measurements and predictions. Additionally, the delivery efficiency of constant flow delivery could be improved upon. While the efficiency was higher than initially expected, finding ways to conserve the iNO delivered during exhalation could result in an improvement in delivery efficiency, thus resulting in less NO escaping into the surrounding environment.

This study focused exclusively on nasal breathing during delivery and did not account for potential changes in delivery during possible oral breathing. While it has been reported that there is the possibility of nasal breathing occurring simultaneously during oral breathing (Rodenstein and Stanescu, 1984), further investigation into this is required. Additionally, this study focused on delivery using adult airway replicas, and conclusions drawn from this research are not necessarily applicable to other age groups. Delivery concentrations and flows will likely be different for infants and adolescents, given their different breathing patterns and the different size and shape of their airways. The experiments outlined in this thesis could be reproduced using upper airway replicas of infants and adolescents.

Pulsed flow of iNO through a nasal cannula could be assessed if the experimental means to produce pulsed delivery characteristics were available. This could be assessed *in vitro* following an adapted methodology similar to this study and a study comparing pulsed and continuous oxygen delivery (Chen *et al.*, 2017). Additionally, following the procedure outlined by Martin *et al.* the NO uptake in the lungs could be modelled using the delivery parameters and results (Martin *et al*., 2014).

Lastly, *in vivo* experiments are recommended to corroborate the feasibility of constant flow iNO delivery through a nasal cannula, and the reported dose delivery. The physiological effects of iNO could not be replicated *in vitro*, so concerns about ventilation-perfusion could be better assessed *in vivo*. While estimates for NO_2 production were provided in Chapter 3, these concentrations could be simply measured *in vivo* with a rapid response analyzer. In addition, intrasubject variability around spontaneous breathing would be measurable *in vivo*; the breathing simulated during this study was mechanical and replicated for a fixed volume, which *in vivo* would change breath-to-breath. Although multiple *in vivo* studies have been conducted for iNO therapy, there are none designed around continuous flow through a nasal cannula. This thesis suggests that clinical application of iNO therapy using this delivery mode may be viable; as such, future *in vivo* studies focused on constant flow delivery through a nasal cannula would be appropriate.

Works Cited

Abman, S.H., 2013. Inhaled Nitric Oxide for the Treatment of Pulmonary Arterial Hypertension, in: Humbert, M., Evgenov, O.V., Stasch, J., (Eds.)Pharmacotherapy of Pulmonary Hypertension, Springer Berlin Heidelberg, Berlin, Heidelberg, pp. 257-276.

American Academy of Pediatrics, 2000. Committee on Fetus and Newborn. Use of inhaled nitric oxide. Pediatrics. 106(2 Pt 1), 344-345.

Ashutosh, K., Phadke, K., Jackson, J.F., Steele, D., 2000. Use of nitric oxide inhalation in chronic obstructive pulmonary disease. Thorax. 55, 109-113.

Auler Júnior, J.O., Carmona, M.J., Bocchi, E.A., Bacal, F., Fiorelli, A.I., Stolf, N.A., Jatene, A.D., 1996. Low doses of inhaled nitric oxide in heart transplant recipients. J. Heart Lung Transplant. 15, 443-450.

Barbera, J.A., Roca, J., 1996. Worsening of pulmonary gas exchange with nitric oxide inhalation in chronic obstructive pulmonary.. Lancet. 347, 436.

Barrington, K.J., Finer, N., Pennaforte, T., Altit, G., 2017. Nitric oxide for respiratory failure in infants born at or near term. Cochrane Database Syst. Rev. 1, CD000399.

Barst, R.J., Agnoletti, G., Fraisse, A., Baldassarre, J., Wessel, D.L., 2010. Vasodilator testing with nitric oxide and/or oxygen in pediatric pulmonary hypertension. Pediatr. Cardiol. 31, 598-606.

Bernard, T.E., 1977. Aspects of on-line digital integration of pulmonary gas transfer. Journal of Applied Physiology Respiratory Environmental and Exercise Physiology. 43, 375-378.

Bhatraju, P., Crawford, J., Hall, M., Lang, J.D., 2015. Inhaled nitric oxide: Current clinical concepts. Nitric Oxide. 50, 114-128.

Bin-Nun, A., Schreiber, M.D., 2008. Role of iNO in the modulation of pulmonary vascular resistance. Journal of Perinatology. 28, S84-S92.

Bylin, G., Lindvall, T., Rehn, T., Sundin, B., 1987. Effects of short-term exposure to ambient nitrogen dioxide concentrations on human bronchial reactivity and lung function. Experientia.Supplementum. 51, 227-230.

Carrigy, N.B., Ruzycki, C.A., Golshahi, L., Finlay, W.H., 2014. Pediatric *In Vitro* and In Silico Models of Deposition via Oral and Nasal Inhalation. Journal of Aerosol Medicine and Pulmonary Drug Delivery. 27, 149-169.

Centers for Disease Control, 1988. Recommendations for occupational safety and health standards. Morbid Mortal Wkly Rep. , 21.

Channick, R.N., Johnson, F.W., Williams, P.J., Auger, W.R., Fedullo, P.F., Moser, K.M., Newhart, J.W., 1996. Pulsed delivery of inhaled nitric oxide to patients with primary pulmonary hypertension: An ambulatory delivery system and initial clinical tests. Chest. 109, 1545-1549.

Chatila, W., Nugent, T., Vance, G., Gaughan, J., Criner, G.J., 2004. The Effects of High-Flow vs Low-Flow Oxygen on Exercise in Advanced Obstructive Airways Disease. Chest. 126, 1108-1115.

Checchia, P., Bronicki, R., Goldstein, B., 2012. Review of Inhaled Nitric Oxide in the Pediatric Cardiac Surgery Setting. Pediatr Cardiol. 33, 493-505.

Chen, J.Z., Katz, I.M., Pichelin, M., Zhu, K., Caillibotte, G., Finlay, W.H., Martin, A.R., 2019. *In Vitro-In Silico* Comparison of Pulsed Oxygen Delivery From Portable Oxygen Concentrators Versus Continuous Flow Oxygen Delivery. Respiratory care. 64, 117-129.

Chen, J.Z., Katz, I.M., Pichelin, M., Zhu, K., Caillibotte, G., Noga, M.L., Finlay, W.H., Martin, A.R., 2017. Comparison of pulsed versus continuous oxygen delivery using realistic adult nasal airway replicas. International journal of chronic obstructive pulmonary disease. 12, 2559-2571.

Clark, R.H., Kueser, T.J., Walker, M.W., Southgate, W.M., Huckaby, J.L., Perez, J.A., Roy, B.J., Keszler, M., Kinsella, J.P., 2000. Low-dose nitric oxide therapy for persistent pulmonary hypertension of the newborn. Clinical Inhaled Nitric Oxide Research Group. N. Engl. J. Med. 342, 469-474.

Cornfield, D.N., Maynard, R.C., deRegnier, R.A., Guiang, S.F., 3, Barbato, J.E., Milla, C.E., 1999. Randomized, controlled trial of low-dose inhaled nitric oxide in the treatment of term and near-term infants with respiratory failure and pulmonary hypertension. Pediatrics. 104, 1089-1094.

Creagh-Brown, B.C., Griffiths, M.J., Evans, T.W., 2009. Bench-to-bedside review: Inhaled nitric oxide therapy in adults. Critical Care. 13, 221.

Cuthbertson, B.H., Stott, S.A., Webster, N.R., Dyar, O.J., Young, J.D., Evans, T.E., Higenbottam, T., Latimer, R., Payen, D., Dellinger, P., 1997. UK guidelines for the use of inhaled nitric oxide therapy in adult ICUs. Intensive Care Med. 23, 1212-1218.

Davidson, D., Barefield, E.S., Kattwinkel, J., Dudell, G., Damask, M., Straube, R., Rhines, J., Chang, C.T., 1998. Inhaled nitric oxide for the early treatment of persistent pulmonary hypertension of the term newborn: a randomized, double-masked, placebo-controlled, dose-response, multicenter study. The I-NO/PPHN Study Group. Pediatrics. 101, 325-334.

Davidson, D., Barefield, E.S., Kattwinkel, J., Dudell, G., Damask, M., Straube, R., Rhines, J., Chang, C.T., I-NO PPHN, S.G., 1999. Safety of withdrawing inhaled nitric oxide therapy in persistent pulmonary hypertension of the newborn. Pediatrics. 104, 231-236.

DiBlasi, R.M., Dupras, D., Kearney, C., Costa, J., Eddie, Griebel, J.L., 2015. Nitric Oxide Delivery by Neonatal Noninvasive Respiratory Support Devices. Respiratory care. 60, 219-230.

DiBlasi, R.M., Myers, T.R., Hess, D.R., 2010. Evidence-based clinical practice guideline: inhaled nitric oxide for neonates with acute hypoxic respiratory failure. Respiratory care. 55, 1717.

Duprez, F., Mashayekhi, S., Cuvelier, G., Legrand, A., Reychler, G., 2018. A New Formula for Predicting the Fraction of Delivered Oxygen During Low-Flow Oxygen Therapy. Respiratory care. 63, 1528-1534.

Finer, N.N., Sun, J.W., Rich, W., Knodel, E., Barrington, K.J., 2001. Randomized, prospective study of low-dose versus high-dose inhaled nitric oxide in the neonate with hypoxic respiratory failure. Pediatrics. 108, 949-955.

Finlay, W.H., 2001. The Mechanics of Inhaled Pharmaceutical Aerosols: An Introduction. Academic Press, San Diego.

Frostell, C.G., Blomqvist, H., Hedenstierna, G., Lundberg, J., Zapol, W.M., 1993. Inhaled nitric oxide selectively reverses human hypoxic pulmonary vasoconstriction without causing systemic vasodilation. Anesthesiology. 78, 427-435.

Frostell, C., Fratacci, M., Wain, J., Jones, R., Zapol, W., 1991. Inhaled Nitric Oxide. A selective pulmonary vasodilator reversing hypoxic pulmonary vasoconstriction. Circulation. 83, 2038-2047.

Fullerton, D.A., McIntyre, R.C., J., 1996. Inhaled nitric oxide: therapeutic applications in cardiothoracic surgery. Ann. Thorac. Surg. 61, 1856-1864.

Germann, P., Ziesche, R., Leitner, C., Roeder, G., Urak, G., Zimpfer, M., Sladen, R., 1998. Addition of Nitric Oxide to Oxygen Improves Cardiopulmonary Function in Patients With Severe COPD. Chest. 114, 29-35.

Ghadimi, K., Rajagopal, S., 2019. Nasally Inhaled Nitric Oxide for Sudden Right-Sided Heart Failure in the Intensive Care Unit: NO Time Like the Present. J. Cardiothorac. Vasc. Anesth. 33, 648-650.

Golshahi, L., Noga, M.L., Thompson, R.B., Finlay, W.H., 2011. *In vitro* deposition measurement of inhaled micrometer-sized particles in extrathoracic airways of children and adolescents during nose breathing. Journal of Aerosol Science. 42, 474-488.

Griffiths, M.J.D., Evans, T.W., 2005. Inhaled Nitric Oxide Therapy in Adults. The New England Journal of Medicine. 353, 2683-2695.

Hajian, B., De Backer, J., Vos, W., Van Holsbeke, C., Ferreira, F., Quinn, D.A., Hufkens, A., Claes, R., De Backer, W., 2016. Pulmonary vascular effects of pulsed inhaled nitric oxide in COPD patients with pulmonary hypertension. International journal of chronic obstructive pulmonary disease. 11, 1533-1541.

Heinonen, E., Hogman, M., Merilainen, P., 2000. Theoretical and experimental comparison of constant inspired concentration and pulsed delivery in NO therapy. Intensive Care Med. 26, 1116-1123.

Hess, D., Ritz, R., Branson, R.D., 1997. Delivery systems for inhaled nitric oxide. Respir. Care Clin. N. Am. 3, 371-410.

Hudgel, D.W., Martin, R.J., Capehart, M., Johnson, B., Hill, P., 1983. Contribution of hypoventilation to sleep oxygen desaturation in chronic obstructive pulmonary disease. J Appl Physiol. 55, 669-677.

Imanaka, H., Hess, D., Kirmse, M., Bigatello, L., M, Kacmarek, R., M, Steudel, W., Hurford, W., E, 1997. Inaccuracies of nitric oxide delivery systems during adult mechanical ventilation. Anesthesiology [0003-3022]. 86, 676-688.

International Organization for Standardization, 2014. Medical electrical equipment. Part 2-67: Particular requirements for basic safety and essential performance of oxygen conserving equipment. , Vol ISO 80601-67:2014(E).

Ivy, D.D., Griebel, J.L., Kinsella, J.P., Abman, S.H., 1998. Acute hemodynamic effects of pulsed delivery of low flow nasal nitric oxide in children with pulmonary hypertension. J. Pediatr. 133, 453-456.

Ivy, D.D., Parker, D., Doran, A., Kinsella, J.P., Abman, S.H., 2003. Acute hemodynamic effects and home therapy using a novel pulsed nasal nitric oxide delivery system in children and young adults with pulmonary hypertension. Am. J. Cardiol. 92, 886-890.

Johnston, H.S., Slentz, L.W., 1951. Oxidation of Nitric Oxide at High Pressures of Reactants. J. Am. Chem. Soc. 73, 2948.

Kanmaz, H.G., Büyüktiryaki, M., Oğuz, ŞS., Dizdar Alyamac, E., Sarı, F.N., Canpolat, F.E., Uras, N., 2017. The Impact of Combined Oral Sildenafil and Inhaled Nitric Oxide for Treating Persistent Pulmonary Hypertension of the Newborn: A Single Center Experience. Gynecology Obstetrics & Reproductive Medicine. 23, 100-104.

Katz, I., Chen, J., Duong, K., Zhu, K., Pichelin, M., Caillibotte, G., Martin, A.R., 2019. Dose variability of supplemental oxygen therapy with open patient interfaces based on *in vitro* measurements using a physiologically realistic upper airway model. Respiratory Research. 20, 149.

Kinsella, J.P., Parker, T.A., Ivy, D.D., Abman, S.H., Kinsella, J.P., Parker, T.A., Ivy, D.D., Abman, S.H., 2003. Noninvasive delivery of inhaled nitric oxide therapy for late pulmonary hypertension in newborn infants with congenital diaphragmatic hernia. J. Pediatr. 142, 397-401.

Kitamukai, O., Sakuma, M., Takahashi, T., Nawata, J., Ikeda, J., Shirato, K., 2002. Hemodynamic effects of inhaled nitric oxide using pulse delivery and continuous delivery systems in pulmonary hypertension. Internal Medicine. 41, 429-434.

Kumar, P., 2014. Use of Inhaled Nitric Oxide in Preterm Infants. Pediatrics. 133, 164-170.

Langer, A., W, Hutcheson, S., Charlton, J., D, McCubbin, J., A, Obrist, P., A, Stoney, C., M, 1985. On-Line Minicomputerized Measurement of Cardiopulmonary Function On a Breath-By-Breath Basis. Psychophysiology. 22, 50-58.

Lindberg, L., Rydgren, G., 1999. Production of nitrogen dioxide during nitric oxide therapy using the Servo Ventilator 300 during volume-controlled ventilation. Acta Anaesthesiol. Scand. 43, 289-294.

Lundin, S., Stenqvist, O., Mang, H., Smithies, M., Frostell, C., 1999. Inhalation of nitric oxide in acute lung injury: Results of a European multicentre study. Intensive Care Med. 25, 911-919.

Lundin, S., Stevqvist, O., 1997. Uptake of inhaled nitric oxide in acute lung injury. Acta anaesthesiologica scandinavica. 41, 818-823.

Luscher, T.F., Vanhoutte, P.M., 1988. Endothelium-dependent responses in human blood vessels. Trends Pharmacol. Sci. 9, 181-184.

Martin, A.R., Jackson, C., Fromont, S., Pont, C., Katz, I.M., Caillobotte, G., 2016. An injection and mixing element for delivery and monitoring of inhaled nitric oxide. Biomedical engineering online. 15, 103.

Martin, A.R., Jackson, C., Katz, I.M., Caillibotte, G., 2014. Variability in uptake efficiency for pulsed versus constant concentration delivery of inhaled nitric oxide. Medical gas research. 4, 1.

Martin, A.R., Moore, C.P., Finlay, W.H., 2018. Models of deposition, pharmacokinetics, and intersubject variability in respiratory drug delivery. Expert Opinion on Drug Delivery. 15, 1175-1188.

McLaughlin, V.V., Archer, S.L., Badesch, D.B., Barst, R.J., Farber, H.W., Lindner, J.R., Mathier, M.A., McGoon, M.D., Park, M.H., Rosenson, R.S., Rubin, L.J., Tapson, V.F., Varga, J., Comm, W., 2009. ACCF/AHA 2009 Expert Consensus Document on Pulmonary Hypertension A Report of the American College of Cardiology Foundation Task Force on Expert Consensus Documents and the American Heart Association. J. Am. Coll. Cardiol. 53, 1573-1619.

Meyer, M., Piiper, J., 1989. Nitric oxide (NO), a new test gas for study of alveolar-capillary diffusion. Eur. Respir. J. 2, 494-496.

Mitchell, R.R., 1979. Incorporating the gas analyzer response time in gas exchange computations. Journal of Applied Physiology Respiratory Environmental and Exercise Physiology. 47, 1118-1122.

No Authors, 1997. Inhaled nitric oxide in full-term and nearly full-term infants with hypoxic respiratory failure. N. Engl. J. Med. 336, 597-604.

Oz, M.C., Ardehali, A., 2004. Collective Review: Perioperative Uses of Inhaled Nitric Oxide in Adults. The heart surgery forum. 7, E584-E589.

Quinn, D on behalf of Bellerophon Therapeutics, 2019. Clinical study of pulsed, inhaled nitric oxide versus placebo in symptomatic subjects with PAH (INOvation-1).

Raja, S.G., Augoustides, J.G., 2004. Treatment of rebound pulmonary hypertension: Why not sildenafil? [3] (multiple letters). Anesthesiology. 101, 1480-1481.

Rasmussen, T.R., Kjaergaard, S.K., Tarp, U., Pedersen, O.F., 1992. Delayed effects of NO2 exposure on alveolar permeability and glutathione peroxidase in healthy humans. Am. Rev. Respir. Dis. 146, 654-659.

Roberts, J.D., Fineman, J.R., Morin, F.C., Shaul, P.W., Rimar, S., Schreiber, M.D., Polin, R.A., Zwass, M.S., Zayek, M.M., Gross, I., Heymann, M.A., Zapol, W.M., 1997. Inhaled nitric oxide and persistent pulmonary hypertension of the newborn. N. Engl. J. Med. 336, 605-610.

Robyn J. Barst, Richard Channick, Ivy Dunbar, Brahm Goldstein, 2012. Clinical perspectives with long-term pulsed inhaled nitric oxide for the treatment of pulmonary arterial hypertension. Pulmonary Circulation. 2, 139-147.

Rodenstein, D., Stanescu, D., 1984. Soft Palate and Oronasal Breathing in Humans. Journal of Applied Physiology.

Schairer, D.O., Chouake, J.S., Nosanchuk, J.D., Friedman, A.J., 2012. The potential of nitric oxide releasing therapies as antimicrobial agents. Virulence. 3, 271-279.

Shapiro, B.A., Peruzzi, W.T., Kozelowski-Templin, R., 1994. Clinical application of blood gases, 5th ed. ed. Mosby.

Smith, D.P., Perez, J.A., 2016. Noninvasive inhaled nitric oxide for persistent pulmonary hypertension of the newborn: A single center experience. Journal of neonatal-perinatal medicine. 9, 211-215.

Taylor, J.R., 1997. An introduction to error analysis : the study of uncertainties in physical measurements, 2nd ed. ed. University Science Books.

Tiep, B., Carter, R., 2008. Oxygen conserving devices and methodologies. Chron Respir Dis. 5, 109-114.

Tremblay, J., Couture, ÉJ., Albert, M., Beaubien-Souligny, W., Elmi-Sarabi, M., Lamarche, Y., Denault, A.Y., 2019. Noninvasive Administration of Inhaled Nitric Oxide and its Hemodynamic Effects in Patients With Acute Right Ventricular Dysfunction. Journal of Cardiothoracic and Vascular Anesthesia. 33, 642-647.

Tsukahara, H., Ishida, T., Mayumi, M., 1999. Gas-phase oxidation of nitric oxide: chemical kinetics and rate constant. Nitric Oxide. 3, 191-198.

Tworetzky, W., Bristow, J., Moore, P., Brook, M., M, Segal, M.R., Brasch, R., C, Hawgood, S., Fineman, J., R, 2001. Inhaled nitric oxide in neonates with persistent pulmonary hypertension. Lancet. 357, 118-20.

US Food and Drug Administration, Centre for Devices and Radiological Health, 2000. Guidance Document for Premarket Notification Submissions for Nitric Oxide Delivery Apparatus, Nitric Oxide Analyzer and Nitrogen Dioxide Analyzer.

Vendettuoli, V., Bellu, R., Zanini, R., Mosca, F., Gagliardi, L., Italian, N.N., 2014. Changes in ventilator strategies and outcomes in preterm infants. Archives Of Disease In Childhood-Fetal And Neonatal Edition. 99, F321-F324.

Vonbank, K., Ziesche, R., Higenbottam, T.W., Stiebellehner, L., Petkov, V., Schenk, P., Germann, P., Block, L.H., 2003. Controlled prospective randomised trial on the effects on pulmonary haemodynamics of the ambulatory long term use of nitric oxide and oxygen in patients with severe COPD. Thorax. 58, 289-293.

Westfelt, U.N., Lundin, S., Stenqvist, O., 1996. Safety aspects of delivery and monitoring of nitric oxide during mechanical ventilation. Acta anaesthesiologica Scandinavica. 40, 302-310.

Westphal, K., Strouhal, U., Hommel, K., Kessler, P., Martens, S., Matheis, G., 1998. Nitric oxide inhalation in acute pulmonary hypertension after cardiac surgery reduces oxygen concentration and improves mechanical ventilation but not mortality. Thorac. Cardiovasc. Surg. 46, 70-73.

Yaacoby-Bianu, K., Gur, M., Toukan, Y., Nir, V., Hakim, F., Geffen, Y., Bentur, L., 2018. Compassionate Nitric Oxide Adjuvant Treatment of Persistent Mycobacterium Infection in Cystic Fibrosis Patients. The Pediatric Infectious Disease Journal. 37, 336-338.

Young, J.D., Roberts, M., Gale, L.B., 1997. Laboratory evaluation of the I-NOvent nitric oxide delivery device. Br J Anaesth. 79, 398-401.

Zapol, W., Yu, B., 2016. Systems and methods for synthesis of nitric oxide.

Appendix A Additional Calculations

A1. Nitrogen dioxide formation

One of the cannulas used for testing in this thesis had a single lumen that had premixed flows of NO (mimicked by CO_2 supply) and O_2 upstream. Given that the present work could not test for NO_2 formation *in vitro* a simple calculation is presented here to determine the maximum amount of NO_2 that could be produced during the time the gases are interacting in the cannula. This time is represented by

$$t = \frac{\frac{\pi(ID)^2 \cdot L}{4}}{\dot{V}_{NO} + \dot{V}_{O2}} \quad \text{[A-1]}$$

where ID is the cannula inner diameter, L is the length of the cannula, $\dot{V}_{NO}$ is the flow rate of NO and $\dot{V}_{O2}$ is the flow rate of O_2.

Following the procedure outlined by Tsukahara *et al.* the rate of NO_2 formation (Tsukahara, Ishida, & Mayumi, 1999) is defined by:

$$\frac{dNO_2}{dt} = 2k \cdot [NO]^2 \cdot [O_2] \quad \text{[A-2]}$$

Given the approximate molar concentrations of NO and O_2 during this time, and assuming NTP conditions, the rate constant k was 7.1 x 10^3 (Johnston and Slentz, 1951). For the high and low flow rates, the maximum NO_2 formed was 0.49 and 0.08 ppm NO_2 respectively. These values each represent 0.21 % and 0.11% of the supplied NO flow respectively which will be further diluted during the intake of room air.

Appendix B Additional Figures

B1. Average tracheal iNO volume

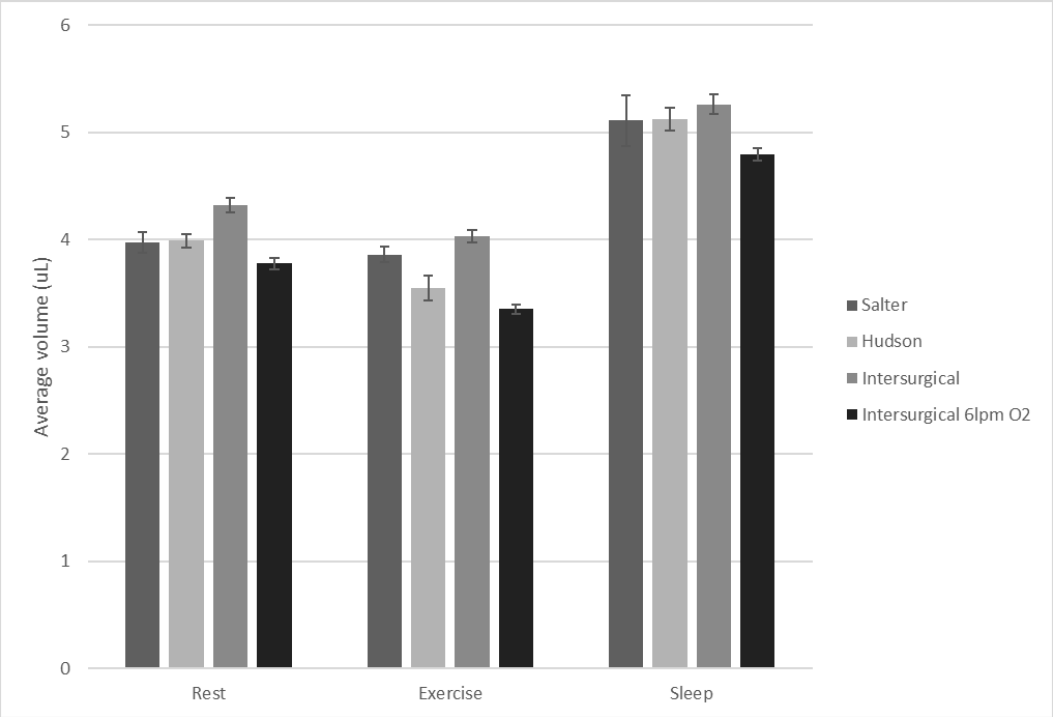

Figure B-1 Average volume of NO per breath at the trachea for 0.2 L/min of 800 ppm NO supply, presented by breathing pattern. The grey columns each represent average tracheal NO volume concentration for 2 L/min supplemental O_2 with different cannulas while the black column represents the volume for 6 L/min supplemental O_2 with an Intersurgical cannula.

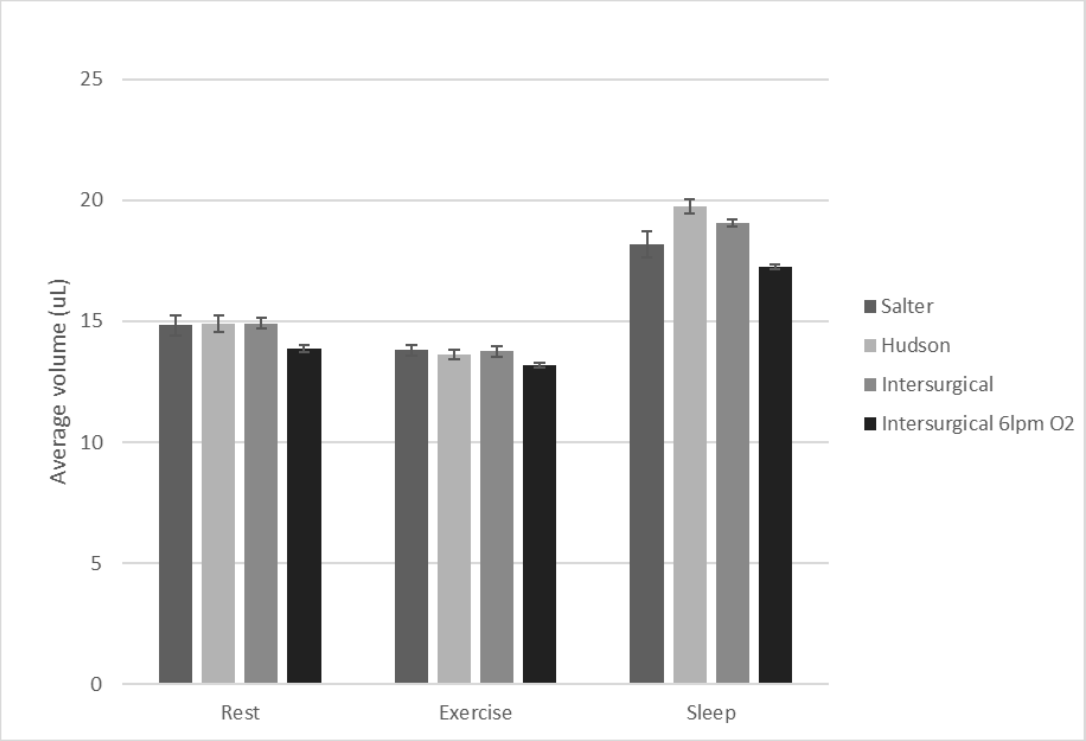

Figure B-2 Average volume of NO per breath at the trachea for 0.8 L/min of 800 ppm NO supply, presented by breathing pattern. The grey columns each represent average tracheal NO volume concentration for 2 L/min supplemental O_2 with different cannulas while the black column represents the volume for 6 L/min supplemental O_2 with an Intersurgical cannula.

B2. Ratio of iNO inhaled during first half of inhalation

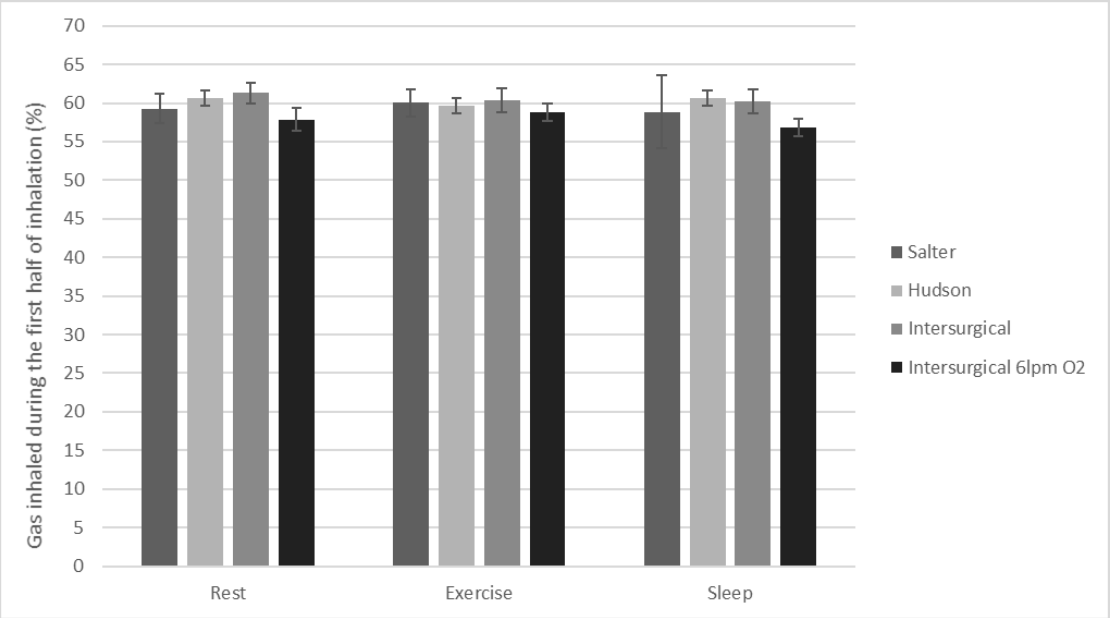

Figure B-3 Ratio of iNO inhaled during first half of inhalation for 0.2 L/min of 800 ppm NO supply, presented by breathing pattern. The grey columns each represent the ratio for 2 L/min supplemental O2 with different cannulas while the black column represents it for 6 L/min supplemental O_2 with an Intersurgical cannula.

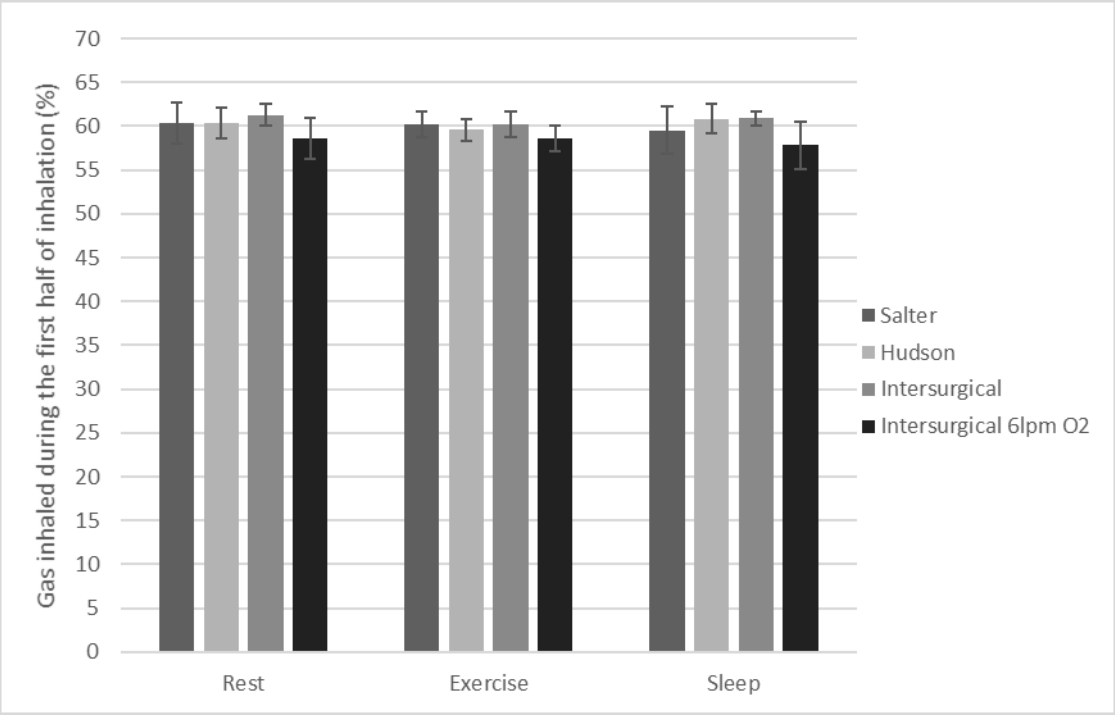

Figure B-4 Ratio of iNO inhaled during first half of inhalation for 0.8 L/min of 800 ppm NO supply, presented by breathing pattern. The grey columns each represent the ratio for 2 L/min supplemental O_2 with different cannulas while the black column represents it for 6 L/min supplemental O_2 with an Intersurgical cannula.

B3. Delivery Efficiency of iNO

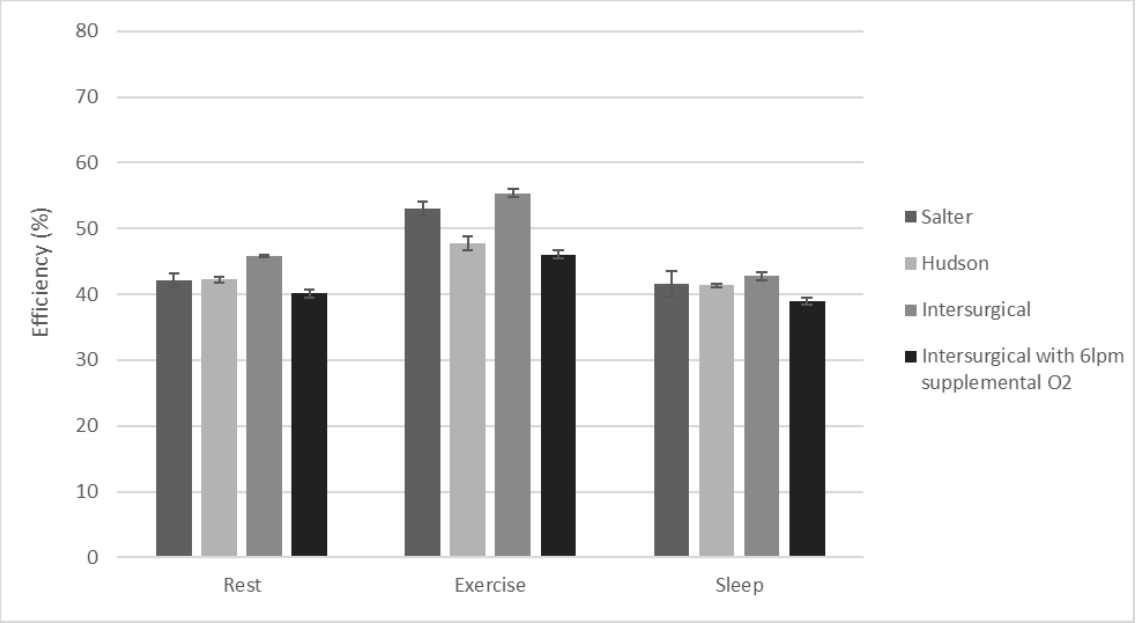

Figure B-5 Delivery efficiency for 0.2 L/min of 800 ppm NO supply, presented by breathing pattern. The grey columns each represent the efficiency for 2 L/min supplemental O_2 with different cannulas while the black column represents it for 6 L/min supplemental O_2 with an Intersurgical cannula.

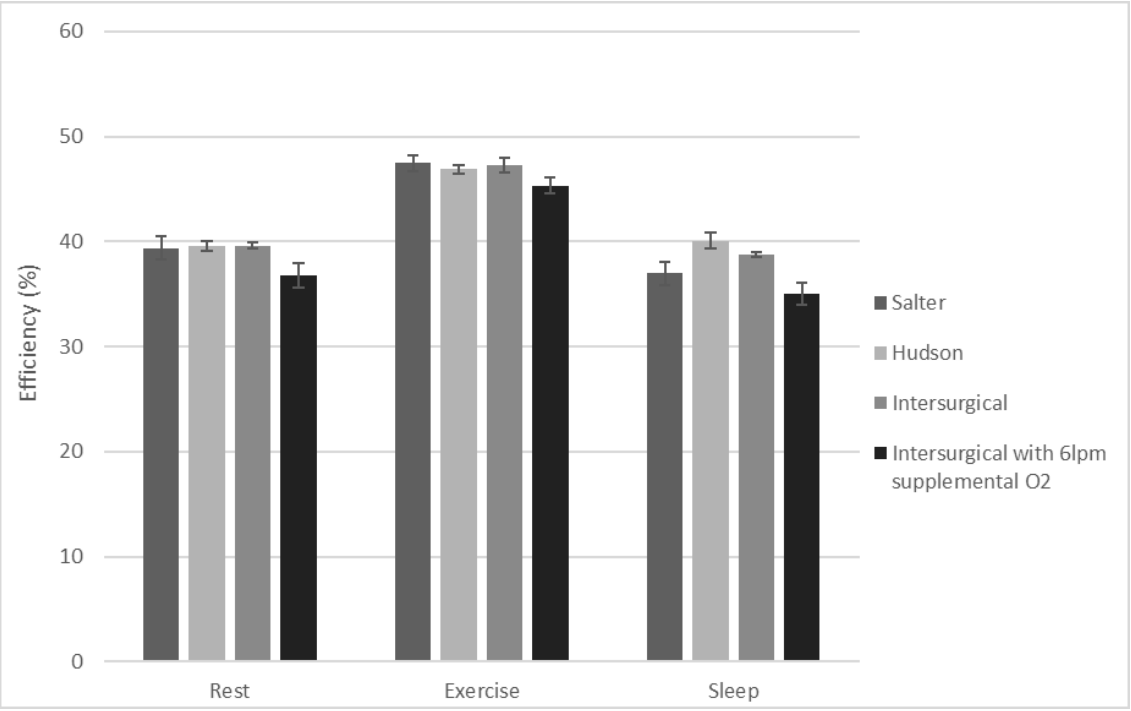

Figure B-6 Delivery efficiency for 0.8 L/min of 800 ppm NO supply, presented by breathing pattern. The grey columns each represent the efficiency for 2 L/min supplemental O_2 with different cannulas while the black column represents it for 6 L/min supplemental O_2 with an Intersurgical cannula.

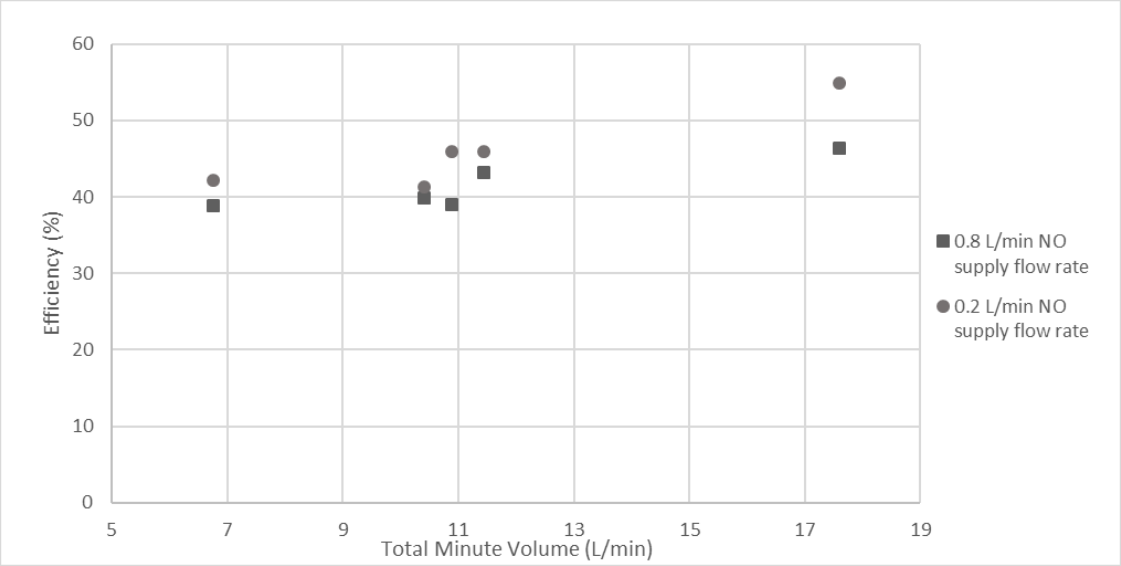

Figure B-7 Delivery efficiency for 0.8 and 0.2 L/min of 800 ppm NO supply with 2 L/min supplemental O_2 through the Intersurgical cannula. Results are presented as a function of the overall minute volume inhaled for during the breathing pattern tested in each condition. The delivery efficiency, and mass flow rate by association, can be observed to increase as the minute volume increases.

B4. Mass flow rate predictions

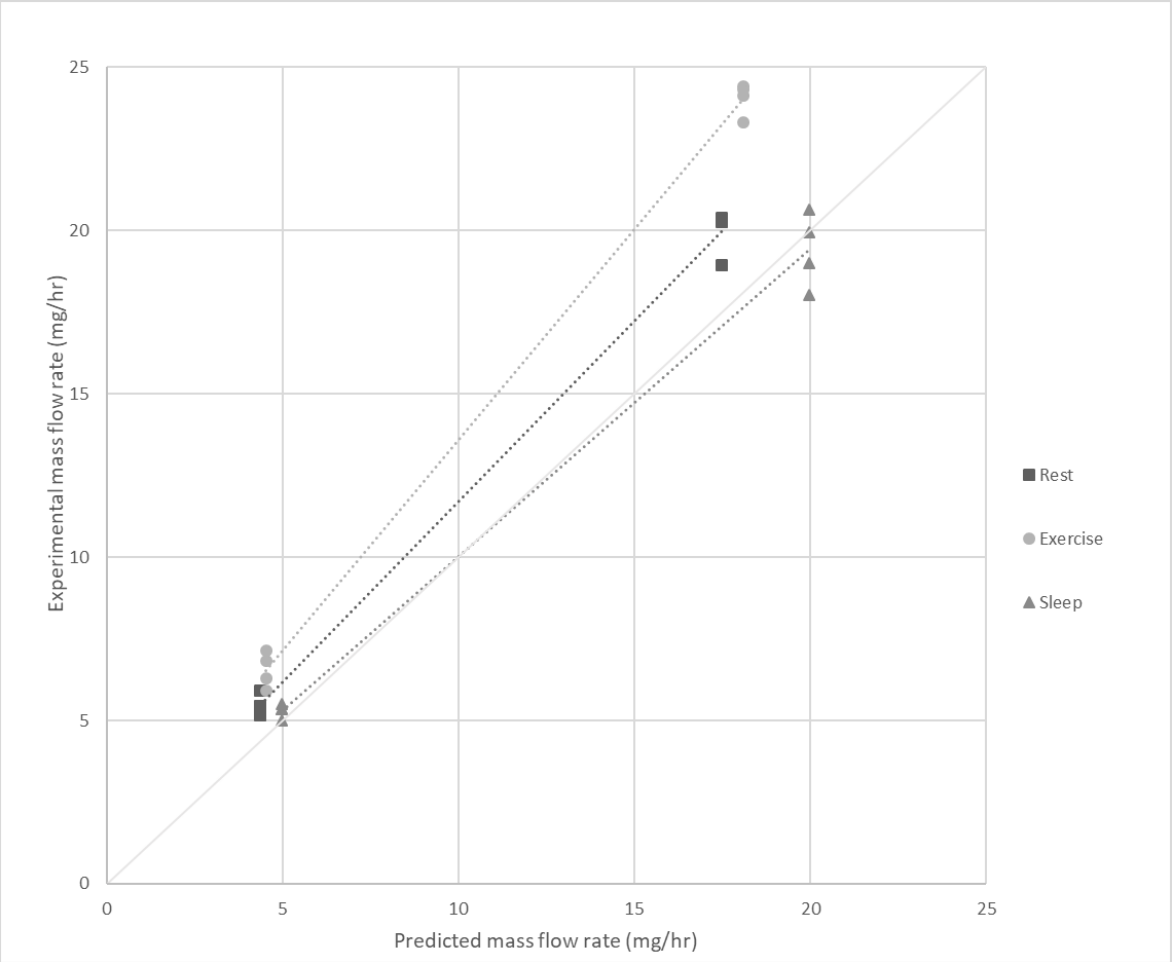

Figure B-8 Differences between the experimental and predicted NO mass flow rate past the trachea, separated by breathing pattern. Measured NO mass flow rate was best predicted for the sleep breathing pattern while rest and exercise were progressively poorly predicted. Sleep had the highest concentrations while exercise had the lowest.

B5. Sample NO waveforms

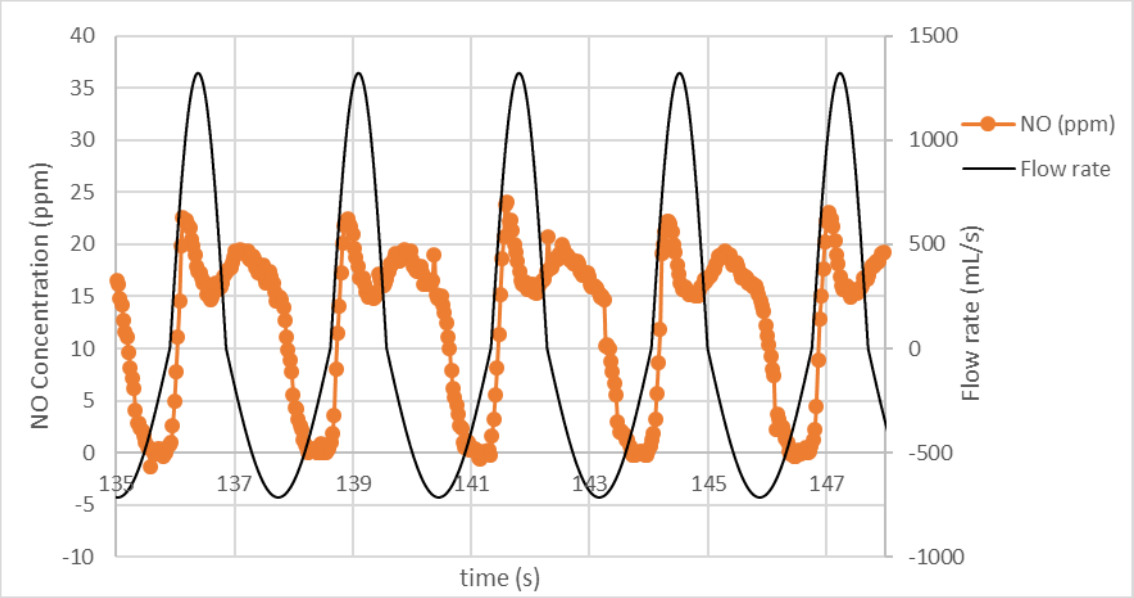

Figure B-9 Sample NO concentration and total flow rate past the trachea recorded during data acquisition process for 0.8 L/min of 800 ppm NO supply during exercise with 2 L/min supplemental O2. NO concentration drops towards zero at the end of each breath as NO that is not absorbed is exhaled.

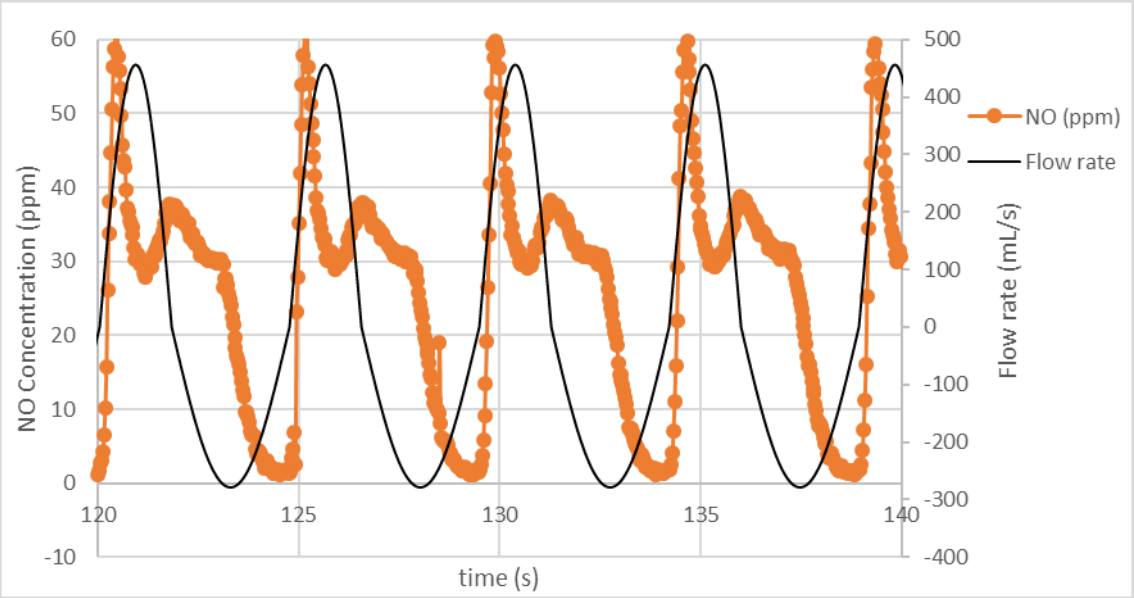

Figure B-10 Sample NO concentration and total flow rate past the trachea recorded during data acquisition process for 0.8 L/min of 800 ppm NO supply during sleep with 2 L/min supplemental O2. The large spike at the start of inhalation is likely due to end-expiratory pooling in the airways.

Appendix C Data Summary

All results displayed in this appendix are averaged over 5 breaths and 3 tests (n=15). Uncertainty for NO concentration represents 1 standard deviation across tests. Uncertainty for mass flow rate, minute volume and η represent propagated error from uncertainty in NO concentration using standard techniques.

C1. Salter cannula with 2 L/min O_2 flow rate

Table C-1 Average results for NO concentration and mass flow rate with the Salter cannula at 2 L/min O2 flow rate

NO supply flow rate (L/min)	Tidal Volume (mL)	Breaths per minute (bpm)	Experimental NO Concentration (ppm)	Predicted NO Concentration (ppm)	Experimental NO mass flow rate (mg/hr)	Predicted NO mass flow rate (mg/hr)
0.8	640	17	23.16±0.66	20	20.26±0.58	17.49
0.8	800	22	17.26±0.27	12.8	24.42±0.38	18.11
0.8	520	13	34.98±1.03	36.71	19.01±0.56	19.95
0.2	640	17	6.2±0.14	5	5.42±0.12	4.37
0.2	800	22	4.82±0.09	3.2	6.82±0.13	4.52
0.2	520	13	9.83±0.45	9.17	5.34±0.24	4.98

Table C-2 Average results for NO delivery efficiency and minute volume with the Salter cannula at 2 L/min O2 flow rate

NO supply flow rate (L/min)	Tidal Volume (mL)	Breaths per minute (bpm)	Efficiency (%)	Experimental NO minute volume (uL/min)	Predicted NO minute volume (uL/min)	Overall minute volume (L/min)
0.8	640	17	39.28±0.49	252.07±7.25	217.6	10.88
0.8	800	22	47±0.69	303.81±4.81	225.28	17.6
0.8	520	13	37.81±0.91	236.52±6.98	248.21	6.76
0.2	640	17	42.52±0.6	67.53±1.57	54.4	10.88
0.2	800	22	53.32±1.14	84.93±1.61	56.32	17.6
0.2	520	13	39.59±0.84	66.46±3.08	62.05	6.76

C2. Hudson cannula with 2 L/min O_2 flow rate

Table C-3 Average results for NO concentration and mass flow rate with the Hudson cannula at 2 L/min O2 flow rate

NO supply flow rate (L/min)	Tidal Volume (mL)	Breaths per minute (bpm)	Experimental NO Concentration (ppm)	Predicted NO Concentration (ppm)	Experimental NO mass flow rate (mg/hr)	Predicted NO mass flow rate (mg/hr)
0.8	640	17	23.27±0.52	20	20.36±0.45	17.49
0.8	800	22	17.04±0.24	12.8	24.11±0.35	18.11
0.8	520	13	37.94±0.57	36.71	20.62±0.3	19.95
0.2	640	17	6.23±0.1	5	5.45±0.08	4.37
0.2	800	22	4.43±0.14	3.2	6.27±0.2	4.52
0.2	520	13	9.84±0.2	9.17	5.35±0.1	4.98

Table C-4 Average results for NO delivery efficiency and minute volume with the Hudson cannula at 2 L/min O2 flow rate

NO supply flow rate (L/min)	Tidal Volume (mL)	Breaths per minute (bpm)	Efficiency (%)	Experimental NO minute volume (uL/min)	Predicted NO minute volume (uL/min)	Overall minute volume (L/min)
0.8	640	17	39.71±0.44	253.27±5.69	217.6	10.88
0.8	800	22	47.5±0.37	299.96±4.36	225.28	17.6
0.8	520	13	40.03±0.75	256.5±3.85	248.21	6.76
0.2	640	17	42.39±0.4	67.82±1.1	54.4	10.88
0.2	800	22	48.78±0.99	78.05±2.54	56.32	17.6
0.2	520	13	41.6±0.25	66.56±1.35	62.05	6.76

C3. Intersurgical cannula with 2 L/min O_2 flow rate

Table C-5 Average results for NO concentration and mass flow rate with the Intersurgical cannula at 2 L/min O2 flow rate

NO supply flow rate (L/min)	Tidal Volume (mL)	Breaths per minute (bpm)	Experimental NO Concentration (ppm)	Predicted NO Concentration (ppm)	Experimental NO mass flow rate (mg/hr)	Predicted NO mass flow rate (mg/hr)
0.8	640	17	23.3±0.36	20	20.38±0.31	17.49
0.8	800	22	17.18±0.3	12.8	24.32±0.42	18.11
0.8	520	13	36.67±0.27	36.71	19.93±0.14	19.95
0.2	640	17	6.75±0.1	5	5.9±0.08	4.37
0.2	800	22	5.03±0.07	3.2	7.12±0.1	4.52
0.2	520	13	10.11±0.17	9.17	5.49±0.09	4.98

Table C-6 Average results for NO delivery efficiency and minute volume with the Intersurgical cannula at 2 L/min O2 flow rate

NO supply flow rate (L/min)	Tidal Volume (mL)	Breaths per minute (bpm)	Efficiency (%)	Experimental NO minute volume (uL/min)	Predicted NO minute volume (uL/min)	Overall minute volume (L/min)
0.8	640	17	38.96±0.3	253.54±3.97	217.6	10.88
0.8	800	22	46.41±0.71	302.52±5.31	225.28	17.6
0.8	520	13	38.91±0.24	247.91±1.86	248.21	6.76
0.2	640	17	45.96±0.16	73.44±1.1	54.4	10.88
0.2	800	22	54.96±0.57	88.65±1.27	56.32	17.6
0.2	520	13	42.18±0.69	68.39±1.16	62.05	6.76

C4. Intersurgical cannula with 6 L/min O_2 flow rate

Table C-7 Average results for NO concentration and mass flow rate with the Intersurgical cannula at 6 L/min O2 flow rate

NO supply flow rate (L/min)	Tidal Volume (mL)	Breaths per minute (bpm)	Experimental NO Concentration (ppm)	Predicted NO Concentration (ppm)	Experimental NO mass flow rate (mg/hr)	Predicted NO mass flow rate (mg/hr)
0.8	640	17	21.64±0.23	20	18.93±0.2	17.49
0.8	800	22	16.48±0.14	12.8	23.32±0.2	18.11
0.8	520	13	33.16±0.17	36.71	18.02±0.09	19.95
0.2	640	17	5.9±0.08	5	5.16±0.07	4.37
0.2	800	22	4.18±0.05	3.2	5.92±0.07	4.52
0.2	520	13	7.49±0.09	9.17	5.01±0.06	4.98

Table C-8 Average results for NO delivery efficiency and minute volume with the Intersurgical cannula at 6 L/min O2 flow rate

NO supply flow rate (L/min)	Tidal Volume (mL)	Breaths per minute (bpm)	Efficiency (%)	Experimental NO minute volume (uL/min)	Predicted NO minute volume (uL/min)	Overall minute volume (L/min)
0.8	640	17	36.8±0.39	235.53±2.55	217.6	10.88
0.8	800	22	45.32±0.39	290.06±2.55	225.28	17.6
0.8	520	13	35.03±0.18	224.22±1.16	248.21	6.76
0.2	640	17	40.13±0.58	64.21±0.93	54.4	10.88
0.2	800	22	46.08±0.6	73.73±0.97	56.32	17.6
0.2	520	13	38.96±0.48	62.34±0.78	62.05	6.76

C5. Intersurgical cannula at 2 L/min O_2 flow rate with varied breathing frequency

Table C-9 Average results for NO concentration and mass flow rate with the Intersurgical cannula at 2 L/min O2 flow rate. Breathing frequency was varied for a fixed breathing ratio and tidal volume implemented above.

NO supply flow rate (L/min)	Tidal Volume (mL)	Breaths per minute (bpm)	Experimental NO Concentration (ppm)	Predicted NO Concentration (ppm)	Experimental NO mass flow rate (mg/hr)	Predicted NO mass flow rate (mg/hr)
0.8	800	13	24.5±0.57	20	20.49±0.47	17.49
0.8	520	22	24.18±0.58	12.8	22.23±0.53	19.55
0.2	800	13	6.35±0.23	36.71	5.31±0.19	4.37
0.2	520	22	6.42±0.08	5	5.91±0.07	4.88

Table C-10 Average results for NO delivery efficiency and minute volume with the Intersurgical cannula at 2 L/min O2 flow rate. Breathing frequency was varied for a fixed breathing ratio and tidal volume implemented above.

NO supply flow rate (L/min)	Tidal Volume (mL)	Breaths per minute (bpm)	Efficiency (%)	Experimental NO minute volume (uL/min)	Predicted NO minute volume (uL/min)	Overall minute volume (L/min)
0.8	800	13	39.82±0.93	254.87±5.95	217.55	10.4
0.8	520	22	43.21±1.04	276.6±6.71	243.22	11.44
0.2	800	13	41.3±1.54	66.09±2.47	54.38	10.4
0.2	520	22	45.95±0.58	73.52±0.94	60.8	11.44

Table C-11 Comparison of all experiments using the Intersurgical cannula with 2 L/min supplemental O2 flow rate with a constant tidal volume and varied breathing frequency.

NO supply flow rate (L/min)	**Tidal Volume, V_T (mL)**	**Breathing Frequency (min^{-1})**	**Experimental NO Concentration (ppm)**	**Experimental NO mass flow rate over time, (mg/hr)**	**Predicted NO mass flow rate over time (mg/hr)**
0.8	800	22	17.2 ± 0.3	24.3 ± 0.4	18.1
0.8	520	13	36.7 ± 0.3	19.9 ± 0.2	20.0
0.8	800	13	24.5 ± 0.6	20.5 ± 0.5	17.5
0.8	520	22	24.2 ± 0.6	22.2 ± 0.5	19.6
0.2	800	22	5 ± 0.1	7.1 ± 0.1	4.5
0.2	520	13	10.1 ± 0.2	5.5 ± 0.1	5.0
0.2	800	13	6.4 ± 0.2	5.3 ± 0.2	4.4
0.2	520	22	6.4 ± 0.1	5.9 ± 0.1	4.9

Appendix D Raw data

D1. Tracheal NO concentration over inhalation with initial breathing patterns

For initial breathing pattern parameters refer to Table 3-1.

Table D-1 Raw data for tracheal NO concentration measured for original breathing patterns. NO was supplied with 2 L/min supplemental O_2. Each row represents a separate test.

Cannula type	NO supply flow rate (L/min)	Breathing pattern	NO Breath 1 (ppm)	NO Breath 2 (ppm)	NO Breath 3 (ppm)	NO Breath 4 (ppm)	NO Breath 5 (ppm)
Salter	0.8	Rest	23.55	22.81	22.89	23.20	23.09
Salter	0.8	Rest	22.33	22.51	22.74	22.61	23.11
Salter	0.8	Rest	24.08	24.28	22.84	24.58	22.92
Salter	0.8	Exercise	17.03	16.71	17.12	17.20	17.40
Salter	0.8	Exercise	17.31	17.22	17.76	17.43	17.36
Salter	0.8	Exercise	17.78	17.18	17.10	17.30	17.03
Salter	0.8	Sleep	37.29	35.16	35.23	35.64	35.67
Salter	0.8	Sleep	34.01	35.07	34.23	34.07	34.05
Salter	0.8	Sleep	34.12	36.94	34.44	34.42	34.50
Salter	0.2	Rest	6.31	6.38	6.22	6.21	6.16
Salter	0.2	Rest	6.08	5.98	6.03	6.10	6.06
Salter	0.2	Rest	6.16	6.29	6.46	6.42	6.25
Salter	0.2	Exercise	4.96	4.94	4.77	4.72	4.85
Salter	0.2	Exercise	4.75	4.80	4.79	4.74	4.66
Salter	0.2	Exercise	4.87	4.94	4.89	4.93	4.78
Salter	0.2	Sleep	9.23	9.41	9.20	9.32	9.70
Salter	0.2	Sleep	9.86	9.72	9.58	10.34	9.83
Salter	0.2	Sleep	9.93	10.16	10.78	10.01	10.40
Hudson	0.8	Rest	23.17	23.61	23.27	23.09	23.67

Hudson	0.8	Rest	22.53	22.37	22.97	22.87	22.99
Hudson	0.8	Rest	24.20	23.85	24.05	23.31	23.24
Hudson	0.8	Exercise	17.36	17.43	17.09	17.32	17.18
Hudson	0.8	Exercise	16.60	16.66	16.85	16.81	17.11
Hudson	0.8	Exercise	16.79	17.10	17.15	17.08	17.10
Hudson	0.8	Sleep	39.01	37.14	37.45	38.04	37.86
Hudson	0.8	Sleep	38.60	38.93	37.21	37.51	37.71
Hudson	0.8	Sleep	37.60	37.71	38.16	38.27	37.97
Hudson	0.2	Rest	6.18	6.15	6.31	6.21	6.20
Hudson	0.2	Rest	6.13	6.19	6.17	6.16	6.29
Hudson	0.2	Rest	6.28	6.51	6.12	6.30	6.32
Hudson	0.2	Exercise	4.31	4.23	4.37	4.33	4.47
Hudson	0.2	Exercise	4.69	4.63	4.68	4.53	4.53
Hudson	0.2	Exercise	4.34	4.39	4.33	4.33	4.37
Hudson	0.2	Sleep	9.73	9.71	9.84	9.83	9.82
Hudson	0.2	Sleep	9.80	10.09	9.89	9.81	10.35
Hudson	0.2	Sleep	9.58	9.78	10.13	9.69	9.66
Intersurgical	0.8	Rest	22.71	22.80	22.94	23.01	23.16
Intersurgical	0.8	Rest	23.63	23.29	23.35	23.21	23.17
Intersurgical	0.8	Rest	23.60	23.71	24.05	23.54	23.39
Intersurgical	0.8	Exercise	17.28	16.89	16.90	16.73	16.58
Intersurgical	0.8	Exercise	17.13	17.12	17.36	17.35	17.10
Intersurgical	0.8	Exercise	17.38	17.49	17.55	17.55	17.42
Intersurgical	0.8	Sleep	37.03	36.91	37.07	36.59	36.61
Intersurgical	0.8	Sleep	36.56	36.16	36.41	36.52	36.81
Intersurgical	0.8	Sleep	36.43	37.08	36.42	36.87	36.63
Intersurgical	0.2	Rest	6.79	6.73	6.74	6.74	6.78
Intersurgical	0.2	Rest	6.56	6.64	6.77	6.86	6.90
Intersurgical	0.2	Rest	6.72	6.90	6.82	6.72	6.58
Intersurgical	0.2	Exercise	4.97	4.94	5.04	4.96	5.06
Intersurgical	0.2	Exercise	5.09	5.00	5.10	5.02	4.94

Intersurgical	0.2	Exercise	5.01	5.19	5.07	5.14	5.02
Intersurgical	0.2	Sleep	10.20	10.04	9.87	9.78	10.03
Intersurgical	0.2	Sleep	10.26	10.01	10.33	10.42	10.28
Intersurgical	0.2	Sleep	10.15	10.11	10.11	10.00	10.16

Table D-2 Raw data for tracheal NO concentration measured for original breathing patterns. NO was supplied with 6 L/min supplemental O_2. Each row represents a separate test.

Cannula type	**NO supply flow rate (L/min)**	**Breathing pattern**	**NO Breath 1 (ppm)**	**NO Breath 2 (ppm)**	**NO Breath 3 (ppm)**	**NO Breath 4 (ppm)**	**NO Breath 5 (ppm)**
Intersurgical	0.8	Rest	21.55	21.37	21.71	21.62	21.37
Intersurgical	0.8	Rest	21.33	21.60	22.05	21.75	21.45
Intersurgical	0.8	Rest	22.13	21.53	21.80	21.71	21.76
Intersurgical	0.8	Exercise	16.37	16.47	16.26	16.54	16.47
Intersurgical	0.8	Exercise	16.56	16.32	16.81	16.52	16.48
Intersurgical	0.8	Exercise	16.34	16.42	16.73	16.42	16.51
Intersurgical	0.8	Sleep	33.35	33.23	33.19	33.25	33.14
Intersurgical	0.8	Sleep	32.94	33.38	33.34	33.38	33.28
Intersurgical	0.8	Sleep	33.07	33.16	32.80	32.97	33.07
Intersurgical	0.2	Rest	5.93	5.95	5.88	5.92	5.86
Intersurgical	0.2	Rest	6.04	6.07	5.96	5.90	5.90
Intersurgical	0.2	Rest	5.80	5.76	5.78	5.87	5.92
Intersurgical	0.2	Exercise	4.23	4.21	4.20	4.19	4.20
Intersurgical	0.2	Exercise	4.07	4.11	4.11	4.21	4.23
Intersurgical	0.2	Exercise	4.18	4.21	4.29	4.21	4.20
Intersurgical	0.2	Sleep	7.60	7.56	7.51	7.57	7.47
Intersurgical	0.2	Sleep	7.45	7.40	7.37	7.40	7.38
Intersurgical	0.2	Sleep	7.69	7.42	7.54	7.58	7.46

D2. Tracheal NO concentration over inhalation with modified breathing patterns

Table D-3 Raw data for tracheal NO concentration measured for modified breathing patterns. For a fixed tidal volume as outlined in table 3-1 the breathing frequency was varied. NO was supplied with 6 L/min supplemental O2. Each row represents a separate test.

Cannula type	NO supply flow rate (L/min)	Breathing pattern	NO Breath 1 (ppm)	NO Breath 2 (ppm)	NO Breath 3 (ppm)	NO Breath 4 (ppm)	NO Breath 5 (ppm)
Intersurgical	0.8	V_T = 0.8 L f = 13 min^{-1}	23.89	25.13	25.00	24.67	25.41
Intersurgical	0.8	V_T = 0.8 L f = 13 min^{-1}	24.24	25.07	24.73	24.33	23.78
Intersurgical	0.8	V_T = 0.8 L f = 13 min^{-1}	23.39	23.91	24.54	24.69	24.83
Intersurgical	0.8	V_T = 0.52 L f = 22 min^{-1}	23.91	23.76	23.75	23.70	23.64
Intersurgical	0.8	V_T = 0.52 L f = 22 min^{-1}	23.67	23.69	24.02	24.16	24.96
Intersurgical	0.8	V_T = 0.52 L f = 22 min^{-1}	25.48	24.58	24.15	24.16	25.10
Intersurgical	0.2	V_T = 0.8 L f = 13 min^{-1}	6.11	6.36	6.45	6.34	6.22
Intersurgical	0.2	V_T = 0.8 L f = 13 min^{-1}	6.13	6.11	6.10	6.41	7.01
Intersurgical	0.2	V_T = 0.8 L f =13 min^{-1}	6.48	6.23	6.30	6.56	6.52
Intersurgical	0.2	V_T = 0.52 L f = 22 min^{-1}	6.30	6.41	6.39	6.44	6.43
Intersurgical	0.2	V_T = 0.52 L f = 22 min^{-1}	6.40	6.56	6.47	6.33	6.32
Intersurgical	0.2	V_T = 0.52 L f = 22 min^{-1}	6.53	6.56	6.48	6.35	6.44